

Bernstein approximation of optimal control problems*

Venanzio Cichella[†], Isaac Kaminer[‡], Claire Walton[‡], Naira Hovakimyan[§], António M. Pascoal[¶]

December 18, 2018

Abstract

Bernstein polynomial approximation to a continuous function has a slower rate of convergence as compared to other approximation methods. *“The fact seems to have precluded any numerical application of Bernstein polynomials from having been made. Perhaps they will find application when the properties of the approximant in the large are of more importance than the closeness of the approximation.”* – has remarked P.J. Davis in his 1963 book Interpolation and Approximation.

This paper presents a direct approximation method for nonlinear optimal control problems with mixed input and state constraints based on Bernstein polynomial approximation. We provide a rigorous analysis showing that the proposed method yields consistent approximations of time continuous optimal control problems. Furthermore, we demonstrate that the proposed method can also be used for costate estimation of the optimal control problems. This latter result leads to the formulation of the Covector Mapping Theorem for Bernstein polynomial approximation. Finally, we explore the numerical and geometric properties of Bernstein polynomials, and illustrate the advantages of the proposed approximation method through several numerical examples.

1 Introduction

Optimal control problems that arise from most engineering applications are in general very complex. Finding a closed-form solution to these problems can be difficult or even impossible, and therefore they must be solved numerically. Numerical methods include indirect and direct methods [1]. Indirect methods solve the problems by converting them into boundary value problems. Then, the solutions are found by solving systems of differential equations. On the other hand, direct methods are based on transcribing optimal control problems into nonlinear programming problems (NLPs) using some discretization scheme [1–4]. These NLPs can be solved using ready-to-use NLP solvers (e.g. MATLAB, SNOPT, etc.) and do not require calculation of costate and adjoint variables as indirect methods do.

A pioneering work in the literature on direct methods is the one of Polak on consistency of approximation theory reported in his book (see [5, Section 3.3]). Borrowing tools from variational analysis, Polak provides a theoretical framework to assess the convergence properties of direct methods. Motivated by the consistency of approximation theory, a wide range of direct methods that use different discretization schemes have been developed, including Euler [5], Runge-Kutta [6], Pseudospectral [7] methods, as well as the method presented in this paper.

Pseudospectral methods are the most popular direct methods nowadays, and they have been applied successfully for solving a wide range of optimization problems, e.g. [7–13]. They offer several advantages over many other discretization methods, mainly owing to their spectral (exponential) rate of convergence.

*This work was supported by AFOSR, ONR, NSF and NASA.

[†]Venanzio Cichella is with the Department of Mechanical Engineering, University of Iowa, Iowa City, 52242 IA venanzio-cichella@uiowa.edu

[‡]Isaac Kaminer and Claire Walton are with the Department of Mechanical and Aerospace Engineering, Naval Postgraduate School, Monterey, CA 93940 {kaminer, clwalton1}@nps.edu

[§]Naira Hovakimyan is with the Department of Mechanical Science and Engineering, University of Illinois at Urbana-Champaign, Urbana, IL 61801 nhovakim@illinois.edu

[¶]António M. Pascoal is with the Institute for Systems and Robotics (ISR), Instituto Superior Tecnico (IST), Univ. Lisbon, Portugal. antoniog@isr.ist.utl.pt

However, as pointed out in [14–17], there is one salient disadvantage associated with these methods. When discretizing the state and/or the input, the constraints are enforced at the discretization nodes; unfortunately, satisfaction of constraints cannot be guaranteed in between the nodes. To avoid violation of the constraints in between the nodes, the order of approximation (number of nodes) can be increased; however, this leads to larger NLPs, which may become computationally expensive and too inefficient to solve. This problem does not limit itself to pseudospectral methods, but it is common to methods that are based on discretization.

This undesirable behaviour becomes obvious, for example, when considering the optimal trajectory generation problem for multi-vehicle missions, where a large number of vehicles have to reach their final destinations by following trajectories that have to guarantee intervehicle separation for safety all the time. Clearly, with a small order of approximation, separation between the trajectories will be hardly satisfied. Increasing the number of nodes will eventually produce spatially separated trajectories, but will also drastically increase the number of collision avoidance constraints and thus also the complexity of the problem.

Pseudospectral methods also suffer from a drawback when dealing with non-smooth optimal control problems. This drawback is mainly related to the well known Gibbs phenomenon [18], common to all approximation methods based on orthogonal polynomials. The Gibbs phenomenon, visible in the form of oscillations, reduces the accuracy of the approximation to first order away from discontinuities and to $\mathcal{O}(1)$ in the neighborhoods of jumps [19]. Several extensions of pseudospectral methods have been developed to deal with this disadvantage and lessen the effect of the Gibbs phenomenon (e.g. [20–22]). The most accurate methods require the location of the discontinuities to be known a priori, which is often impractical or difficult. Other methods are based on the estimation of these locations, which could result in inefficiency or ill conditioning of the discretized problem, especially when the number of discontinuities is large and unknown.

The present article proposes a direct method based on Bernstein approximation. Bernstein approximants have several nice properties. First of all, the approximants converge uniformly to the functions that they approximate – and so do their derivatives [23, Chapter 3]. This, as we will discuss later, is useful for derivation of convergence properties of the proposed computational method. Moreover, Bernstein polynomials behave well, even when the functions being approximated are non-smooth. In fact, as demonstrated in [24], the Gibbs phenomenon does not occur when approximating piecewise smooth, monotone functions with both left and right derivatives at every point by Bernstein polynomials. As a result, the proposed method based on Bernstein approximation lends itself to problems that have discontinuous states and/or controls, e.g. bang-bang optimal control problems (see also [25]). Finally, due to their favorable geometric properties (see [23, Chapter 5]) Bernstein polynomials afford computationally efficient algorithms for the computation of state and input constraints for the whole time interval where optimization takes place, and not only at discretization points (see [16, 26]). Hence, with the proposed approach the solutions can be guaranteed to be feasible and satisfy the constraints for all times, while retaining the computational efficiency of methods based on discretization.

“There is a price that must be paid for these beautiful approximation properties: the convergence of the Bernstein polynomials is very slow.” – wrote P.J. Davis in his 1963 book *Interpolation and Approximation* [27]. He continues: *“This fact seems to have precluded any numerical application of Bernstein polynomials from having been made. Perhaps they will find application when the properties of the approximant in the large are of more importance than the closeness of the approximation.”* In fact, the slow convergence of the Bernstein approximation implies that the approach proposed in the present paper is outperformed by, for example, pseudospectral methods in terms of convergence rate. This is not surprising, since the choice of nodes and the interpolating polynomials in the pseudospectral methods is dictated by approximation accuracy and convergence speed, while sacrificing satisfaction of constraints in between the nodes. On the other hand, our approach prioritizes constraint satisfaction at the expense of a slower convergence rate.

The paper is structured as follows: in Section 2 we present the notation and the mathematical results, which will be used later in the paper. Section 3 introduces the optimal control problem of interest and some related assumptions. Section 4 presents the NLP method based on Bernstein approximation that approximates the optimal control problem. Section 5 demonstrates that the proposed approximation method yields approximate results that converges uniformly to the optimal solution. In Section 6 we derive the KarushKuhnTucker (KKT) conditions associated with the NLP. Section 7 compares these conditions to the first order optimality conditions for the original optimal control problem and states the Covector Mapping

Theorem for Bernstein approximation. Numerical examples are discussed in Section 8. The paper ends with conclusions in Section 9.

2 Notation and mathematical background

Vector valued functions are denoted by bold letters, $\mathbf{x}(t) = [x_1(t), \dots, x_n(t)]^\top$, while vectors are denoted by bold letters with an upper bar, $\bar{\mathbf{x}} = [x_1, \dots, x_n]^\top \in \mathbb{R}^n$. The symbol \mathcal{C}^r denotes the space of functions with r continuous derivatives. \mathcal{C}_n^r denotes the space of n -vector valued functions in \mathcal{C}^r . $\|\cdot\|$ denotes the Euclidean norm, $\|\bar{\mathbf{x}}\| = \sqrt{x_1^2 + \dots + x_n^2}$.

2.1 Bernstein polynomials

The Bernstein basis polynomials of degree N are defined as

$$b_{j,N}(t) = \binom{N}{j} t^j (1-t)^{N-j}, \quad t \in [0, 1],$$

for $j = 0, \dots, N$, with

$$\binom{N}{j} = \frac{N!}{j!(N-j)!}.$$

They were originally introduced by the mathematician Sergei Natanovich Bernstein in 1912 to facilitate a constructive proof of the Weierstrass approximation theorem [28]. An N th order Bernstein polynomial $x_N : [0, 1] \rightarrow \mathbb{R}$ is a linear combination of $N + 1$ Bernstein basis polynomials of order N , i.e.

$$x_N(t) = \sum_{j=0}^N \bar{x}_j b_{j,N}(t), \quad t \in [0, 1],$$

where $\bar{x}_j \in \mathbb{R}$, $j = 0, \dots, N$, are referred to as Bernstein coefficients (also known as control points). For the sake of generality, and with a slight abuse of terminology, in this paper we extend the definition of a Bernstein polynomial given above to a vector of N th order polynomials $\mathbf{x}_N : [0, 1] \rightarrow \mathbb{R}^n$ expressed in the following form

$$\mathbf{x}_N(t) = \sum_{j=0}^N \bar{\mathbf{x}}_{j,N} b_{j,N}(t), \quad t \in [0, 1], \quad (1)$$

where $\bar{\mathbf{x}}_{0,N}, \dots, \bar{\mathbf{x}}_{N,N}$ are n -dimensional Bernstein coefficients.

Bernstein polynomials were popularized by Pierre Bézier in the early 1960s as useful tools for geometric design (Bézier used Bernstein polynomials to design the shape of the cars at the Renault company in France), and are now widely used in computer graphics, animations and type fonts such as postscript fonts and true type fonts. For this reason, the Bernstein polynomial introduced in Equation (1) is often referred to as a Bézier curve, especially when used to describe a spatial curve.

Bernstein polynomials possess favorable geometric and numerical properties that can be exploited in many application domains. For an extensive review on Bernstein polynomials and their properties the reader is referred to [23]. The derivative and integral of a Bernstein polynomial $\mathbf{x}_N(t)$ can be easily computed as

$$\dot{\mathbf{x}}_N(t) = N \sum_{j=0}^{N-1} (\bar{\mathbf{x}}_{j+1,N} - \bar{\mathbf{x}}_{j,N}) b_{j,N-1}(t)$$

and

$$\int_0^1 \mathbf{x}_N(t) dt = w \sum_{j=0}^N \bar{\mathbf{x}}_{j,N}, \quad w = \frac{1}{N+1}, \quad (2)$$

respectively. Bernstein polynomials can be used to approximate smooth functions. Consider a n -vector valued function $\mathbf{x} : [0, 1] \rightarrow \mathbb{R}^n$. The N th order *Bernstein approximation* of $\mathbf{x}(t)$ is a vector of Bernstein polynomials $\mathbf{x}_N(t)$ computed as in (1) with $\bar{\mathbf{x}}_{j,N} = \mathbf{x}(t_j)$ and $t_j = \frac{j}{N}$ for all $j = 0, \dots, N$. Namely,

$$\mathbf{x}_N(t) = \sum_{j=0}^N \mathbf{x}(t_j) b_{j,N}(t), \quad t_j = \frac{j}{N}. \quad (3)$$

The following results hold for Bernstein approximations.

Lemma 1 (Uniform convergence of Bernstein approximation) *Let $\mathbf{x}(t) \in \mathcal{C}_n^0$ on $[0, 1]$, and $\mathbf{x}_N(t)$ be computed as in Equation (3). Then, for arbitrary order of approximation $N \in \mathbb{Z}^+$, the Bernstein approximation $\mathbf{x}_N(t)$ satisfies*

$$\|\mathbf{x}_N(t) - \mathbf{x}(t)\| \leq C_0 W_x(N^{-\frac{1}{2}}),$$

where C_0 is a positive constant satisfying $C_0 < 5n/4$, and $W_x(\cdot)$ is the modulus of continuity of $\mathbf{x}(t)$ in $[0, 1]$ [29–31]. Moreover, if $\mathbf{x}(t) \in \mathcal{C}_n^1$, then

$$\|\dot{\mathbf{x}}_N(t) - \dot{\mathbf{x}}(t)\| \leq C_1 W_{x'}(N^{-\frac{1}{2}}),$$

where C_1 is a positive constant satisfying $C_1 < 9n/4$ and $W_{x'}(\cdot)$ is the modulus of continuity of $\dot{\mathbf{x}}(t)$ in $[0, 1]$ [32]. ■

Lemma 2 [33] *Assume $\mathbf{x}(t) \in \mathcal{C}_n^{r+2}$, $r \geq 0$, and let $\mathbf{x}_N(t)$ be computed as in Equation (3). Let $\mathbf{x}^{(r)}(t)$ denote the r th derivative of $\mathbf{x}(t)$. Then, the following inequalities hold for all $t \in [0, 1]$:*

$$\begin{aligned} \|\mathbf{x}_N(t) - \mathbf{x}(t)\| &\leq \frac{C_0}{N} \\ &\vdots \\ \|\mathbf{x}_N^{(r)}(t) - \mathbf{x}^{(r)}(t)\| &\leq \frac{C_r}{N}, \end{aligned}$$

where C_0, \dots, C_r are independent of N . ■

Lemma 3 *If $\mathbf{x}(t) \in \mathcal{C}_n^0$ on $[0, 1]$, then we have*

$$\left\| \int_0^1 \mathbf{x}(t) dt - w \sum_{j=0}^N \mathbf{x}\left(\frac{j}{N}\right) \right\| \leq C_I W_x(N^{-\frac{1}{2}})$$

with $w = \frac{1}{N+1}$, where $C_I > 0$ is independent of N . Moreover, if $\mathbf{x}(t) \in \mathcal{C}_n^2$, then

$$\left\| \int_0^1 \mathbf{x}(t) dt - w \sum_{j=0}^N \mathbf{x}\left(\frac{j}{N}\right) \right\| \leq \frac{C_I}{N}.$$
■

The Lemma above follows directly from Lemmas 1 and 2 and Equation (2).

The following properties of Bernstein polynomials are relevant to this paper.

Property 1 (End point values) *The Bernstein polynomial given by Equation (1) satisfies $\mathbf{x}_N(0) = \bar{\mathbf{x}}_{0,N}$ and $\mathbf{x}_N(1) = \bar{\mathbf{x}}_{N,N}$. Moreover, the tangent of a Bernstein polynomial at the initial and final points lies on the vectors $\bar{\mathbf{x}}_{1,N} - \bar{\mathbf{x}}_{0,N}$ and $\bar{\mathbf{x}}_{N,N} - \bar{\mathbf{x}}_{N-1,N}$, respectively. A graphical depiction of this property is illustrated in Figure 1a. □*

Property 2 (Convex hull) *A Bernstein polynomial is completely contained in the convex hull of its Bernstein coefficients (see Figure 1b).*

□

Property 3 (de Casteljau Algorithm) *The de Casteljau algorithm is an efficient and numerically stable recursive method to evaluate a Bernstein polynomial at any given point. The de Casteljau algorithm is also used to split a Bernstein polynomial into two independent ones. Given an N th order Bernstein polynomial $\mathbf{x}_N : [0, 1] \rightarrow \mathbb{R}^d$, and a scalar $t_{\text{div}} \in [0, 1]$, the Bernstein polynomial at t_{div} can be computed using the following recursive relation*

$$\begin{aligned}\bar{\mathbf{x}}_{i,N}^{[0]} &= \bar{\mathbf{x}}_{i,N}, \quad i = 0, \dots, N \\ \bar{\mathbf{x}}_{i,N}^{[j]} &= \bar{\mathbf{x}}_{i,N}^{[j-1]}(1 - t_{\text{div}}) + \bar{\mathbf{x}}_{i+1,N}^{[j-1]}t_{\text{div}}, \quad i = 0, \dots, N - j, \quad j = 1, \dots, N.\end{aligned}$$

Then, the Bernstein polynomial evaluated at t_{div} is given by

$$\mathbf{x}_N(t_{\text{div}}) = \bar{\mathbf{x}}_{0,N}^{[N]}.$$

Moreover, the Bernstein polynomial can be subdivided at t_{div} into two N th order Bernstein polynomials with Bernstein coefficients

$$\bar{\mathbf{x}}_{0,N}^{[0]}, \bar{\mathbf{x}}_{0,N}^{[1]}, \dots, \bar{\mathbf{x}}_{0,N}^{[N]}, \quad \text{and} \quad \bar{\mathbf{x}}_{0,N}^{[N]}, \bar{\mathbf{x}}_{1,N}^{[N-1]}, \dots, \bar{\mathbf{x}}_{N,N}^{[0]}.$$

Figure 1c depicts a 2D curve defined by an 5th order Bernstein polynomial (with Bernstein coefficients described by blue circles). The curve is subdivided into two 5th order Bernstein polynomials, each with Bernstein coefficients described by black and red circles.

□

Property 4 (Minimum distance) *The minimum distance between two Bernstein polynomials $\mathbf{f}_N(t)$ and $\mathbf{g}_N(t)$, with $t \in [0, 1]$, namely*

$$\min_{t_a, t_b \in [0, 1]} \|\mathbf{f}_N(t_a) - \mathbf{g}_N(t_b)\|, \quad \arg \min_{t_a, t_b \in [0, 1]} \|\mathbf{f}_N(t_a) - \mathbf{g}_N(t_b)\| \quad (4)$$

can be efficiently computed by exploiting the convex-hull property and the de Casteljau algorithm [23], in combination with the Gilbert-Johnson-Keerthi (GJK) distance algorithm [34]. The latter is widely used in computer graphics and video games to compute the minimum distance between convex shapes. In [26] the authors propose an iterative procedure that uses the above tools to compute (4) within a desired tolerance. This procedure is extremely useful for motion planning applications to efficiently compute the spatial clearance between two paths, or between a path and an obstacle. For example, the minimum distance between the 2D Bernstein polynomial and the point depicted in Figure 1d is computed in less than 5 ms using an implementation in MATLAB, while the minimum distance between the 3D Bernstein polynomials depicted in Figure 1e is computed in less than 30 ms. The same procedure can also be employed to compute the extrema (maximum and minimum) of a Bernstein polynomial [35].

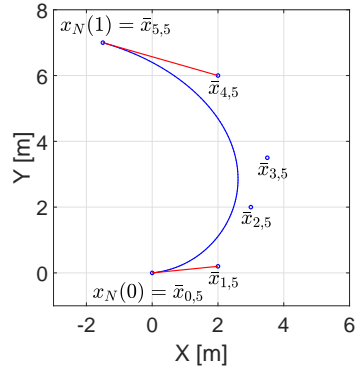
□

3 Problem formulation

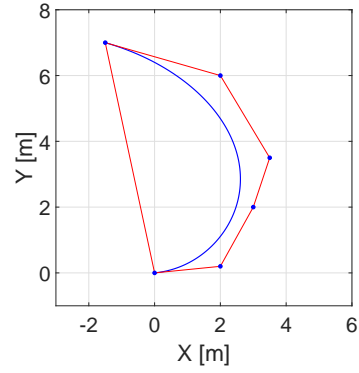
This paper considers the following optimal control problem:

Problem 1 (Problem P) *Determine $\mathbf{x} : [0, 1] \rightarrow \mathbb{R}^{n_x}$ and $\mathbf{u} : [0, 1] \rightarrow \mathbb{R}^{n_u}$ that minimize*

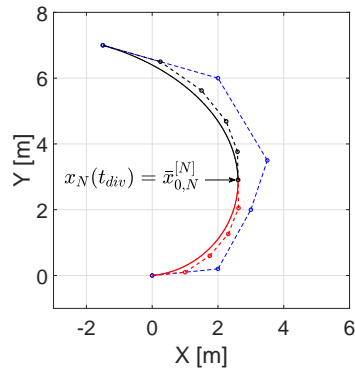
$$I(\mathbf{x}(t), \mathbf{u}(t)) = E(\mathbf{x}(0), \mathbf{x}(1)) + \int_0^1 F(\mathbf{x}(t), \mathbf{u}(t))dt, \quad (5)$$



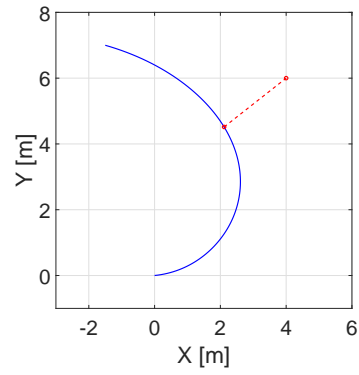
(a) End point values property.



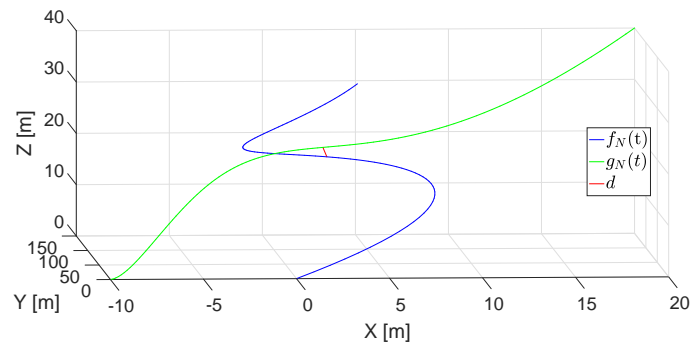
(b) Convex hull property.



(c) de Casteljau algorithm.



(d) Minimum distance to a point.



(e) Distance between two 3D Bernstein polynomials

Figure 1: 2D and 3D spatial curves defined by Bernstein polynomials.

subject to

$$\dot{\mathbf{x}} = \mathbf{f}(\mathbf{x}(t), \mathbf{u}(t)), \quad \forall t \in [0, 1], \quad (6)$$

$$\mathbf{e}(\mathbf{x}(0), \mathbf{x}(1)) = \mathbf{0}, \quad (7)$$

$$\mathbf{h}(\mathbf{x}(t), \mathbf{u}(t)) \leq \mathbf{0}, \quad \forall t \in [0, 1], \quad (8)$$

where $E : \mathbb{R}^{n_x} \times \mathbb{R}^{n_x} \rightarrow \mathbb{R}$ and $F : \mathbb{R}^{n_x} \times \mathbb{R}^{n_u} \rightarrow \mathbb{R}$ are the terminal and running costs, respectively, $\mathbf{f} : \mathbb{R}^{n_x} \times \mathbb{R}^{n_u} \rightarrow \mathbb{R}^{n_x}$ describes the system dynamics, $\mathbf{e} : \mathbb{R}^{n_x} \times \mathbb{R}^{n_x} \rightarrow \mathbb{R}^{n_e}$ is the vector of boundary conditions, and $\mathbf{h} : \mathbb{R}^{n_x} \times \mathbb{R}^{n_u} \rightarrow \mathbb{R}^{n_h}$ is the vector of state and input constraints. ∇

The following assumptions hold:

Assumption 1 E , F , \mathbf{f} , \mathbf{e} , and \mathbf{h} are Lipschitz continuous with respect to their arguments.

Assumption 2 Problem P admits optimal solutions $\mathbf{x}^*(t)$ and $\mathbf{u}^*(t)$ that satisfy $\mathbf{x}^*(t) \in \mathcal{C}_{n_x}^1$ and $\mathbf{u}^*(t) \in \mathcal{C}_{n_u}^0$.

4 Bernstein approximation of Problem P

The purpose of this section is to formulate a discretized version of Problem P , here referred to as Problem P_N , where N denotes the *order of approximation*. This requires that we approximate the input and state functions, the cost function, the system dynamics, and the equality and inequality constraints in Problem P .

First, consider the following N th order vectors of Bernstein polynomials:

$$\mathbf{x}_N(t) = \sum_{j=0}^N \bar{\mathbf{x}}_{j,N} b_{j,N}(t), \quad \mathbf{u}_N(t) = \sum_{j=0}^N \bar{\mathbf{u}}_{j,N} b_{j,N}(t), \quad (9)$$

with $\mathbf{x}_N : [0, 1] \rightarrow \mathbb{R}^{n_x}$, $\mathbf{u}_N : [0, 1] \rightarrow \mathbb{R}^{n_u}$, $\bar{\mathbf{x}}_{j,N} \in \mathbb{R}^{n_x}$ and $\bar{\mathbf{u}}_{j,N} \in \mathbb{R}^{n_u}$. Let $\bar{\mathbf{x}}_N \in \mathbb{R}^{n_x \times (N+1)}$ and $\bar{\mathbf{u}}_N \in \mathbb{R}^{n_u \times (N+1)}$ be defined as

$$\bar{\mathbf{x}}_N = [\bar{\mathbf{x}}_{0,N}, \dots, \bar{\mathbf{x}}_{N,N}], \quad \bar{\mathbf{u}}_N = [\bar{\mathbf{u}}_{0,N}, \dots, \bar{\mathbf{u}}_{N,N}].$$

Let $0 = t_0 < t_1 < \dots < t_N = 1$ be a set of equidistant *time nodes*, i.e. $t_j = \frac{j}{N}$. Then Problem P_N can be stated as follows:

Problem 2 (Problem P_N) Determine $\bar{\mathbf{x}}_N$ and $\bar{\mathbf{u}}_N$ that minimize

$$I_N(\bar{\mathbf{x}}_N, \bar{\mathbf{u}}_N) = E(\mathbf{x}_N(0), \mathbf{x}_N(t_N)) + w \sum_{j=0}^N F(\mathbf{x}_N(t_j), \mathbf{u}_N(t_j)), \quad (10)$$

subject to

$$\|\dot{\mathbf{x}}_N(t_j) - \mathbf{f}(\mathbf{x}_N(t_j), \mathbf{u}_N(t_j))\| \leq \delta_P^N, \quad \forall j = 0, \dots, N, \quad (11)$$

$$\mathbf{e}(\mathbf{x}_N(0), \mathbf{x}_N(t_N)) = \mathbf{0}, \quad (12)$$

$$\mathbf{h}(\mathbf{x}_N(t_j), \mathbf{u}_N(t_j)) \leq \delta_P^N \mathbf{1}, \quad \forall j = 0, \dots, N, \quad (13)$$

where $w = \frac{1}{N+1}$, and δ_P^N is a small positive number that depends on N and converges uniformly to 0, i.e. $\lim_{N \rightarrow \infty} \delta_P^N = 0$. ∇

Remark 1 Compared to the constraints of Problem P , the dynamic and inequality constraints given by Equations (11) and (13) are relaxed. Motivated by previous work on consistency of approximation theory [5], the bound δ_P^N , referred to as relaxation bound, is introduced to guarantee that Problem P_N has a feasible solution. As it will become clear later, the relaxation bound can be made arbitrarily small by choosing a sufficiently large order of approximation N . Furthermore, note that when $N \rightarrow \infty$, then the right hand sides of Equations (11) and (13) equal to zero, i.e. the difference between the constraints imposed by Problems P and P_N vanishes.

5 Feasibility and consistency of Problem P_N

The outcome of Problem P_N is a set of optimal Bernstein coefficients $\bar{\mathbf{x}}_N^*$ and $\bar{\mathbf{u}}_N^*$ that determine the vectors of Bernstein polynomials $\mathbf{x}_N^*(t)$ and $\mathbf{u}_N^*(t)$, i.e.

$$\mathbf{x}_N^*(t) = \sum_{j=0}^N \bar{\mathbf{x}}_{j,N}^* b_{j,N}(t), \quad \mathbf{u}_N^*(t) = \sum_{j=0}^N \bar{\mathbf{u}}_{j,N}^* b_{j,N}(t). \quad (14)$$

Now we address the following theoretical issues:

1. existence of a feasible solution to Problem P_N ,
2. convergence of the pair $(\mathbf{x}_N^*(t), \mathbf{u}_N^*(t))$ to the optimal solution of Problem P , given by $(\mathbf{x}^*(t), \mathbf{u}^*(t))$.

The main results of this section are summarized in Theorems 1 and 2 below.

Theorem 1 (Feasibility) *Let*

$$\delta_P^N = C_P \max\{W_{x'}(N^{-\frac{1}{2}}), W_x(N^{-\frac{1}{2}}), W_u(N^{-\frac{1}{2}})\}, \quad (15)$$

where C_P is a positive constant independent of N , and $W_{x'}(\cdot)$, $W_x(\cdot)$ and $W_u(\cdot)$ are the moduli of continuity of $\dot{\mathbf{x}}(t)$, $\mathbf{x}(t)$ and $\mathbf{u}(t)$, respectively. Then Problem P_N is feasible for arbitrary order of approximation $N \in \mathbb{Z}^+$. ■

Proof: Let $\mathbf{x}(t)$ and $\mathbf{u}(t)$ be a feasible solution for Problem P , which exists by Assumption 2. Let us define the Bernstein coefficients

$$\bar{\mathbf{x}}_{k,N} = \mathbf{x}(t_k), \quad \bar{\mathbf{u}}_{k,N} = \mathbf{u}(t_k), \quad \forall k \in \{0, \dots, N\}, \quad (16)$$

and the resulting vectors of Bernstein polynomials as

$$\mathbf{x}_N(t) = \sum_{j=0}^N \bar{\mathbf{x}}_{j,N} b_{j,N}(t), \quad \mathbf{u}_N(t) = \sum_{j=0}^N \bar{\mathbf{u}}_{j,N} b_{j,N}(t). \quad (17)$$

In what follows, we show that the above polynomials satisfy the constraints in (11), (12) and (13), with δ_P^N defined in Equation (15), thus proving Theorem 1.

Equations (16) and (17), together with Lemma 1 and Assumption 2, imply that $\mathbf{x}_N(t)$, $\dot{\mathbf{x}}_N(t)$ and $\mathbf{u}_N(t)$ converge uniformly to $\mathbf{x}(t)$, $\dot{\mathbf{x}}(t)$ and $\mathbf{u}(t)$, respectively. More precisely, for all $t \in [0, 1]$ from Lemma 1 we have

$$\begin{aligned} \|\mathbf{x}_N(t) - \mathbf{x}(t)\| &\leq C_x W_x(N^{-\frac{1}{2}}), \\ \|\mathbf{u}_N(t) - \mathbf{u}(t)\| &\leq C_u W_u(N^{-\frac{1}{2}}), \\ \|\dot{\mathbf{x}}_N(t) - \dot{\mathbf{x}}(t)\| &\leq C_{x'} W_{x'}(N^{-\frac{1}{2}}), \end{aligned} \quad (18)$$

where $C_x < 5n_x/4$, $C_u < 5n_u/4$ and $C_{x'} < 9n_x/4$ (see Lemma 1). To prove that the dynamic constraint is satisfied, we add and subtract the term $\dot{\mathbf{x}}(t_k) - \mathbf{f}(\mathbf{x}(t_k), \mathbf{u}(t_k))$ from the left hand side of Equation (11), which yields

$$\begin{aligned} \|\dot{\mathbf{x}}_N(t_k) - \mathbf{f}(\mathbf{x}_N(t_k), \mathbf{u}_N(t_k))\| &\leq \|\dot{\mathbf{x}}_N(t_k) - \dot{\mathbf{x}}(t_k)\| + \|\dot{\mathbf{x}}(t_k) - \mathbf{f}(\mathbf{x}(t_k), \mathbf{u}(t_k))\| \\ &\quad + \|\mathbf{f}(\mathbf{x}_N(t_k), \mathbf{u}_N(t_k)) - \mathbf{f}(\mathbf{x}(t_k), \mathbf{u}(t_k))\|. \end{aligned}$$

The second term on the right hand side of the inequality above is zero (see Equation (6)). Using Equation (18) and the fact that \mathbf{f} is Lipschitz (see Assumption 1) with Lipschitz constant L_f , we get

$$\begin{aligned} \|\dot{\mathbf{x}}_N(t_k) - \mathbf{f}(\mathbf{x}_N(t_k), \mathbf{u}_N(t_k))\| &\leq C_{x'} W_{x'}(N^{-\frac{1}{2}}) + L_f \left(C_x W_x(N^{-\frac{1}{2}}) + C_u W_u(N^{-\frac{1}{2}}) \right) \\ &\leq (C_{x'} + L_f(C_x + C_u)) \max(W_{x'}(N^{-\delta}), W_x(N^{-\delta}), W_u(N^{-\delta})). \end{aligned}$$

Thus, the dynamic constraint in Equation (11) is satisfied with δ_P^N given by Equation (15).

Using a similar argument, the satisfaction of the constraint in Equation (13) follows easily by Assumption 1, namely that \mathbf{h} is Lipschitz, i.e.

$$\begin{aligned} \mathbf{h}(\mathbf{x}_N(t_j), \mathbf{u}_N(t_j)) &\leq \mathbf{h}(\mathbf{x}(t_j), \mathbf{u}(t_j)) + \|\mathbf{h}(\mathbf{x}_N(t_j), \mathbf{u}_N(t_j)) - \mathbf{h}(\mathbf{x}(t_j), \mathbf{u}(t_j))\| \\ &\leq \|\mathbf{h}(\mathbf{x}_N(t_j), \mathbf{u}_N(t_j)) - \mathbf{h}(\mathbf{x}(t_j), \mathbf{u}(t_j))\| \\ &\leq L_h(C_x + C_u) \max(W_x(N^{-\delta}), W_u(N^{-\delta})). \end{aligned}$$

Finally, using the end point value property of Bernstein polynomials, i.e. Property 1 in Section 2, we have $\mathbf{x}_N(0) = \bar{\mathbf{x}}_{0,N}$ and $\mathbf{x}_N(1) = \bar{\mathbf{x}}_{N,N}$, which by definition implies that $\mathbf{e}(\mathbf{x}_N(0), \mathbf{x}_N(1)) = \mathbf{e}(\mathbf{x}(0), \mathbf{x}(1)) = \mathbf{0}$, thus proving Equation (12). ♠

Corollary 1 *If the optimal state $\mathbf{x}^*(t)$ and control $\mathbf{u}^*(t)$ solutions to Problem P exist and satisfy $\dot{\mathbf{x}}^*(t) \in \mathcal{C}_{n_x}^2$ and $\mathbf{u}^*(t) \in \mathcal{C}_{n_u}^2$ in $[0, 1]$, then Theorem 1 holds with $\delta_P^N = C_P N^{-1}$, where C_P is a positive constant independent of N .* ■

Proof: The proof of Corollary 1 follows easily by applying Lemma 2 to the proof of Theorem 1. ♠

Remark 2 *From the definition of δ_P^N in Theorem 1 (and Corollary 1), it follows that for any arbitrarily small scalar $\epsilon_P > 0$ there exists N_1 such that for all $N \geq N_1$, we have $\delta_P^N \leq \epsilon_P$. In other words, the relaxation bound in Problem P_N can be made arbitrarily small by choosing sufficiently large N , while retaining the feasibility result (Theorem 1 and Corollary 1).*

Theorem 2 (Consistency) *Let $\{(\bar{\mathbf{x}}_N^*, \bar{\mathbf{u}}_N^*)\}_{N=N_1}^\infty$ be a sequence of optimal solutions to Problem P_N , and $\{(\mathbf{x}_N^*(t), \mathbf{u}_N^*(t))\}_{N=N_1}^\infty$ be a sequence of Bernstein polynomials, given by (14). Assume $\{(\mathbf{x}_N^*(t), \mathbf{u}_N^*(t))\}_{N=N_1}^\infty$ has a uniform accumulation point, i.e.*

$$\lim_{N \rightarrow \infty} (\mathbf{x}_N^*(t), \mathbf{u}_N^*(t)) = (\mathbf{x}^\infty(t), \mathbf{u}^\infty(t)), \quad \forall t \in [0, 1], \quad (19)$$

and assume that $\dot{\mathbf{x}}^\infty(t)$ and $\mathbf{u}^\infty(t)$ are continuous on $[0, 1]$. Then $(\mathbf{x}^\infty(t), \mathbf{u}^\infty(t))$ is an optimal solution for Problem P. ■

Proof: This proof is divided into three steps: (1) we prove that $(\mathbf{x}^\infty(t), \mathbf{u}^\infty(t))$ is a feasible solution to Problem P; (2) we show that

$$\lim_{N \rightarrow \infty} I_N(\bar{\mathbf{x}}_N^*, \bar{\mathbf{u}}_N^*) = I(\mathbf{x}^\infty(t), \mathbf{u}^\infty(t)); \quad (20)$$

(3) we prove that $(\mathbf{x}^\infty(t), \mathbf{u}^\infty(t))$ is an optimal solution of Problem P, i.e.

$$I(\mathbf{x}^\infty(t), \mathbf{u}^\infty(t)) = I(\mathbf{x}^*(t), \mathbf{u}^*(t)).$$

Step (1). First, we show that $(\mathbf{x}^\infty(t), \mathbf{u}^\infty(t))$ satisfies the dynamic constraint of Problem P:

$$\dot{\mathbf{x}}^\infty(t) - \mathbf{f}(\mathbf{x}^\infty(t), \mathbf{u}^\infty(t)) = \mathbf{0}.$$

We show this by contradiction. Assume that the above equality does not hold. Then there exists t' , such that

$$\|\dot{\mathbf{x}}^\infty(t') - \mathbf{f}(\mathbf{x}^\infty(t'), \mathbf{u}^\infty(t'))\| > 0. \quad (21)$$

Since the nodes $\{t_k\}_{k=0}^N$, $t_k = \frac{k}{N}$ are dense in $[0, 1]$, there exists a sequence of indices $\{k_N\}_{N=0}^\infty$ such that

$$\lim_{N \rightarrow \infty} t_{k_N} = t'.$$

Then, from continuity of $\dot{\mathbf{x}}^\infty(t)$, $\mathbf{x}^\infty(t)$ and $\mathbf{u}^\infty(t)$, the left hand side of Equation (21) satisfies

$$\|\dot{\mathbf{x}}^\infty(t') - \mathbf{f}(\mathbf{x}^\infty(t'), \mathbf{u}^\infty(t'))\| = \lim_{N \rightarrow \infty} \|\dot{\mathbf{x}}_N^*(t_{k_N}) - \mathbf{f}(\mathbf{x}_N^*(t_{k_N}), \mathbf{u}_N^*(t_{k_N}))\|.$$

However, the dynamic constraint in Problem P_N is

$$\|\dot{\mathbf{x}}_N^*(t_{k_N}) - \mathbf{f}(\mathbf{x}_N^*(t_{k_N}), \mathbf{u}_N^*(t_{k_N}))\| \leq \delta_P^N,$$

which implies that

$$\lim_{N \rightarrow \infty} \|\dot{\mathbf{x}}_N^*(t_{k_N}) - \mathbf{f}(\mathbf{x}_N^*(t_{k_N}), \mathbf{u}_N^*(t_{k_N}))\| = 0.$$

The above result contradicts Equation (21), thus proving that $(\mathbf{x}^\infty(t), \mathbf{u}^\infty(t))$ satisfies the dynamic constraint in Equation (6). The equality and inequality constraints in (12) and (13) follow easily by an identical argument.

Step (2). To prove that Equation (20) is satisfied we need to show the following:

$$\lim_{N \rightarrow \infty} w \sum_{j=0}^N F(\mathbf{x}_N^*(t_j), \mathbf{u}_N^*(t_j)) = \int_0^1 F(\mathbf{x}^\infty(t), \mathbf{u}^\infty(t)) dt, \quad (22)$$

and

$$\lim_{N \rightarrow \infty} E(\mathbf{x}_N^*(0), \mathbf{x}_N^*(t_N)) = E(\mathbf{x}^\infty(0), \mathbf{x}^\infty(1)). \quad (23)$$

Using Lemma 3, together with the Lipschitz assumption on F (see Assumption 1) and the continuity of $\mathbf{x}^\infty(t)$ and $\mathbf{u}^\infty(t)$, we get

$$\lim_{N \rightarrow \infty} w \sum_{j=0}^N F(\mathbf{x}^\infty(t_j), \mathbf{u}^\infty(t_j)) = \int_0^1 F(\mathbf{x}^\infty(t), \mathbf{u}^\infty(t)) dt.$$

Finally, applying the convergence assumption given by Equation (19), the result in Equation (22) follows. Similarly, using the Lipschitz assumption on E , one can show that Equation (23) holds, thus completing the proof of Step (2).

Step (3). Finally, it remains to show that

$$I(\mathbf{x}^\infty(t), \mathbf{u}^\infty(t)) = I(\mathbf{x}^*(t), \mathbf{u}^*(t)).$$

First, recall that $\mathbf{x}^*(t)$ and $\mathbf{u}^*(t)$ are optimal solutions of Problem P , while $\bar{\mathbf{x}}_N^*$ and $\bar{\mathbf{u}}_N^*$ are optimal solutions of Problem P_N . Let $\tilde{\mathbf{x}}_{k,N} = \mathbf{x}^*(t_k)$, $\tilde{\mathbf{u}}_{k,N} = \mathbf{u}^*(t_k)$, $\forall k \in \{1, \dots, N\}$ and

$$\tilde{\mathbf{x}}_N = [\tilde{\mathbf{x}}_{0,N}, \dots, \tilde{\mathbf{x}}_{N,N}], \quad \tilde{\mathbf{u}}_N = [\tilde{\mathbf{u}}_{0,N}, \dots, \tilde{\mathbf{u}}_{N,N}].$$

Following an argument similar to the one in the proof of Theorem 1, one can show that there exists N_1 such that for any $N \geq N_1$ the pair $(\tilde{\mathbf{x}}_N, \tilde{\mathbf{u}}_N)$ is a feasible solution of Problem P_N . Moreover, an argument similar to the one in the proof of Step (2) yields

$$\lim_{N \rightarrow \infty} I_N(\tilde{\mathbf{x}}_N, \tilde{\mathbf{u}}_N) = I(\mathbf{x}^*(t), \mathbf{u}^*(t)). \quad (24)$$

Then we have

$$I(\mathbf{x}^*(t), \mathbf{u}^*(t)) \leq I(\mathbf{x}^\infty(t), \mathbf{u}^\infty(t)) = \lim_{N \rightarrow \infty} I_N(\bar{\mathbf{x}}_N^*, \bar{\mathbf{u}}_N^*) \leq \lim_{N \rightarrow \infty} I_N(\tilde{\mathbf{x}}_N, \tilde{\mathbf{u}}_N). \quad (25)$$

The last inequality, combined with (24), gives

$$I(\mathbf{x}^*(t), \mathbf{u}^*(t)) = I(\mathbf{x}^\infty(t), \mathbf{u}^\infty(t)),$$

which completes the proof of Theorem 2. ♠

6 Costate estimation for Problem P using Bernstein approximation

6.1 First order optimality conditions of Problem P

We start by deriving the first order necessary conditions for Problem P . Let $\boldsymbol{\lambda}(t) : [0, 1] \rightarrow \mathbb{R}^{n_x}$ be the costate trajectory, and let $\boldsymbol{\mu}(t) : [0, 1] \rightarrow \mathbb{R}^{n_h}$ and $\boldsymbol{\nu} \in \mathbb{R}^{n_e}$ be the multipliers. By defining the Lagrangian of the Hamiltonian (also known as the D-form [36]) as

$$\mathcal{L}(\mathbf{x}(t), \mathbf{u}(t), \boldsymbol{\lambda}(t), \boldsymbol{\mu}(t)) = \mathcal{H}(\mathbf{x}(t), \mathbf{u}(t), \boldsymbol{\lambda}(t)) + \boldsymbol{\mu}^\top(t) \mathbf{h}(\mathbf{x}(t), \mathbf{u}(t)),$$

where the Hamiltonian \mathcal{H} is given by

$$\mathcal{H}(\mathbf{x}(t), \mathbf{u}(t), \boldsymbol{\lambda}(t)) = F(\mathbf{x}(t), \mathbf{u}(t)) + \boldsymbol{\lambda}^\top(t) \mathbf{f}(\mathbf{x}(t), \mathbf{u}(t)),$$

the dual of Problem P can be formulated as follows [36].

Problem 3 (Problem P_λ) Determine $\mathbf{x}(t)$, $\mathbf{u}(t)$, $\boldsymbol{\lambda}(t)$, $\boldsymbol{\mu}(t)$ and $\boldsymbol{\nu}$ that for all $t \in [0, 1]$ satisfy Equations (6), (7), (8) and

$$\boldsymbol{\mu}^\top(t) \mathbf{h}(\mathbf{x}(t), \mathbf{u}(t)) = 0, \quad \boldsymbol{\mu}(t) \geq 0, \quad (26)$$

$$\dot{\boldsymbol{\lambda}}^\top(t) + \mathcal{L}_x(\mathbf{x}(t), \mathbf{u}(t), \boldsymbol{\lambda}(t), \boldsymbol{\mu}(t)) = \dot{\boldsymbol{\lambda}}^\top(t) + F_x(\mathbf{x}(t), \mathbf{u}(t)) + \boldsymbol{\lambda}^\top(t) \mathbf{f}_x(\mathbf{x}(t), \mathbf{u}(t)) + \boldsymbol{\mu}^\top(t) \mathbf{h}_x(\mathbf{x}(t), \mathbf{u}(t)) = 0, \quad (27)$$

$$\boldsymbol{\lambda}^\top(0) = -\boldsymbol{\nu}^\top \mathbf{e}_{x(0)}(\mathbf{x}(0), \mathbf{x}(1)) - E_{x(0)}(\mathbf{x}(0), \mathbf{x}(1)), \quad (28)$$

$$\boldsymbol{\lambda}^\top(1) = \boldsymbol{\nu}^\top \mathbf{e}_{x(1)}(\mathbf{x}(0), \mathbf{x}(1)) + E_{x(1)}(\mathbf{x}(0), \mathbf{x}(1)), \quad (29)$$

$$\mathcal{L}_u(\mathbf{x}(t), \mathbf{u}(t), \boldsymbol{\lambda}(t), \boldsymbol{\mu}(t)) = \boldsymbol{\lambda}^\top(t) \mathbf{f}_u(\mathbf{x}(t), \mathbf{u}(t)) + F_u(\mathbf{x}(t), \mathbf{u}(t)) + \boldsymbol{\mu}^\top(t) \mathbf{h}_u(\mathbf{x}(t), \mathbf{u}(t)) = 0. \quad (30)$$

▽

In the above problem, subscripts are used to denote partial derivatives, e.g. $F_x(\mathbf{x}, \mathbf{u}) = \frac{\partial}{\partial \mathbf{x}} F(\mathbf{x}, \mathbf{u})$.

The following assumptions are imposed onto Problem P_λ .

Assumption 3 $E, F, \mathbf{f}, \mathbf{e}$ and \mathbf{h} are continuously differentiable with respect to their arguments, and their gradients are Lipschitz continuous over the domain.

Assumption 4 Solutions $\mathbf{x}^*(t)$, $\mathbf{u}^*(t)$, $\boldsymbol{\lambda}^*(t)$, $\boldsymbol{\mu}^*(t)$ and $\boldsymbol{\nu}^*$ of Problem P_λ exist and satisfy $\mathbf{x}^*(t) \in \mathcal{C}_{n_x}^1$, $\mathbf{u}^*(t) \in \mathcal{C}_{n_u}^0$, $\boldsymbol{\lambda}^*(t) \in \mathcal{C}_{n_x}^1$ and $\boldsymbol{\mu}^*(t) \in \mathcal{C}_{n_h}^0$ in $[0, 1]$.

Remark 3 Notice that Problem P_λ implicitly assumes the absence of pure state constraints in Problem P . If the inequality constraint in Equation (8) is independent of $\mathbf{u}(t)$, then the costate $\boldsymbol{\lambda}(t)$ must also satisfy the following jump condition [36]:

$$\boldsymbol{\lambda}(t_e^-) = \boldsymbol{\lambda}(t_e^+) + \mathbf{h}_{x(t_e)}^\top \boldsymbol{\eta},$$

where t_e is the entry or exit time into a constrained arc in which the inequality constraint is active, t_e^- and t_e^+ denote the left-hand side and right-hand side limits of the trajectory, respectively, and $\boldsymbol{\eta}$ is a constant covector. For simplicity, the theoretical results that will be presented in Section 7 do not consider the jump conditions above, i.e., the inequality constraints are dependent on $\mathbf{u}(t)$. Nevertheless, numerical examples will be presented in Section 8 showing the applicability of the discretization method to pure state-constrained problems.

6.2 KKT conditions of Problem P_N

Let us introduce the following N th order Bernstein polynomials:

$$\boldsymbol{\lambda}_N(t) = \sum_{j=0}^N \bar{\boldsymbol{\lambda}}_{j,N} b_{j,N}(t), \quad \boldsymbol{\mu}_N(t) = \sum_{j=0}^N \bar{\boldsymbol{\mu}}_{j,N} b_{j,N}(t), \quad (31)$$

with $\boldsymbol{\lambda}_N : [0, 1] \rightarrow \mathbb{R}^{n_x}$, $\boldsymbol{\mu}_N : [0, 1] \rightarrow \mathbb{R}^{n_h}$, $\bar{\boldsymbol{\lambda}}_{j,N} \in \mathbb{R}^{n_x}$ and $\bar{\boldsymbol{\mu}}_{j,N} \in \mathbb{R}^{n_h}$, and the vector $\bar{\boldsymbol{\nu}} \in \mathbb{R}^{n_e}$. Finally, let $\bar{\boldsymbol{\lambda}}_N \in \mathbb{R}^{n_x \times (N+1)}$ and $\bar{\boldsymbol{\mu}}_N \in \mathbb{R}^{n_h \times (N+1)}$ be defined as

$$\bar{\boldsymbol{\lambda}}_N = [\bar{\boldsymbol{\lambda}}_{0,N}, \dots, \bar{\boldsymbol{\lambda}}_{N,N}], \quad \bar{\boldsymbol{\mu}}_N = [\bar{\boldsymbol{\mu}}_{0,N}, \dots, \bar{\boldsymbol{\mu}}_{N,N}].$$

With the above notation, the Lagrangian for problem P_N can be written as

$$\begin{aligned} \mathcal{L}_N = & E(\mathbf{x}_N(0), \mathbf{x}_N(t_N)) + w \sum_{j=0}^N F(\mathbf{x}_N(t_j), \mathbf{u}_N(t_j)) + \sum_{j=0}^N \boldsymbol{\lambda}_N^\top(t_j) (-\dot{\mathbf{x}}_N(t_j) + \mathbf{f}(\mathbf{x}_N(t_j), \mathbf{u}_N(t_j))) \\ & + \sum_{j=0}^N \boldsymbol{\mu}_N^\top(t_j) \mathbf{h}(\mathbf{x}_N(t_j), \mathbf{u}_N(t_j)) + \bar{\boldsymbol{\nu}}^\top \mathbf{e}(\mathbf{x}_N(0), \mathbf{x}_N(t_N)). \end{aligned}$$

Then the dual of Problem P_N can be stated as follows:

Problem 4 (Problem $P_{N\lambda}$) Determine $\bar{\mathbf{x}}_N$, $\bar{\mathbf{u}}_N$, $\bar{\boldsymbol{\lambda}}_N$, $\bar{\boldsymbol{\mu}}_N$ and $\bar{\boldsymbol{\nu}}$ that satisfy the primal feasibility conditions, namely Equations (11), (12) and (13), the complementary slackness and dual feasibility conditions

$$\begin{aligned} \|\boldsymbol{\mu}_N^\top(t_k) \mathbf{h}(\mathbf{x}_N(t_k), \mathbf{u}_N(t_k))\| &\leq N^{-1} \delta_D^N, \\ \boldsymbol{\mu}_N(t_k) &\geq -N^{-1} \delta_D^N \mathbf{1}, \quad \forall k = 0, \dots, N, \end{aligned} \quad (32)$$

and the stationarity conditions

$$\left\| \frac{\partial \mathcal{L}_N}{\partial \bar{\mathbf{x}}_{k,N}} \right\| \leq \delta_D^N, \quad \left\| \frac{\partial \mathcal{L}_N}{\partial \bar{\mathbf{u}}_{k,N}} \right\| \leq \delta_D^N, \quad \forall k = 0, \dots, N, \quad (33)$$

where δ_D^N is a small positive number that depends on N and satisfies $\lim_{N \rightarrow \infty} \delta_D^N = 0$. ▽

At this point one might expect results similar to the ones in Section 5, i.e. feasibility (Theorem 1) and consistency (Theorem 2). Nevertheless, similarly to most results on costate estimation [37–39], this is not the case, and additional conditions must be added to Equations (11)–(13), (32) and (33) in order to obtain consistent approximations of the solutions of Problem P_λ . These conditions, often referred to as *closure conditions* in the literature, are given as follows:

$$\left\| \frac{\boldsymbol{\lambda}_N^\top(0)}{w} + \bar{\boldsymbol{\nu}}^\top \mathbf{e}_{x(0)}(\mathbf{x}_N(0), \mathbf{x}_N(t_N)) + E_{x(0)}(\mathbf{x}_N(0), \mathbf{x}_N(t_N)) \right\| \leq \delta_D^N \quad (34)$$

$$\left\| \frac{\boldsymbol{\lambda}_N^\top(t_N)}{w} - \bar{\boldsymbol{\nu}}^\top \mathbf{e}_{x(1)}(\mathbf{x}_N(0), \mathbf{x}_N(t_N)) - E_{x(1)}(\mathbf{x}_N(0), \mathbf{x}_N(t_N)) \right\| \leq \delta_D^N. \quad (35)$$

In other words, the closure conditions are constraints that must be added to Problem $P_{N\lambda}$ so that the solution of this problem approximates the solution of Problem P_λ . We notice that the conditions given above are discrete approximations of the conditions given by Equations (28) and (29). With this setup, we define the following problem:

Problem 5 (Problem $P_{N\lambda}^{clos}$) Determine $\bar{\mathbf{x}}_N$, $\bar{\mathbf{u}}_N$, $\bar{\boldsymbol{\lambda}}_N$, $\bar{\boldsymbol{\mu}}_N$ and $\bar{\boldsymbol{\nu}}$ that satisfy the primal feasibility conditions, namely Equations (11), (12) and (13), the complementary slackness and dual feasibility conditions (32), the stationarity conditions (33), and the closure conditions (34) and (35). ▽

The solution of Problem $P_{N\lambda}^{clos}$ presents a set of optimal Bernstein coefficients $\bar{\mathbf{x}}_N^*$, $\bar{\mathbf{u}}_N^*$, $\bar{\boldsymbol{\lambda}}_N^*$, $\bar{\boldsymbol{\mu}}_N^*$ (which determine the Bernstein polynomials $\mathbf{x}_N^*(t)$, $\mathbf{u}_N^*(t)$, $\boldsymbol{\lambda}_N^*(t)$ and $\boldsymbol{\mu}_N^*(t)$) and a vector $\bar{\boldsymbol{\nu}}^*$.

7 Feasibility and consistency of Problem $P_{N\lambda}^{clos}$

The objective of this section is to investigate the ability of the solutions of Problem $P_{N\lambda}^{clos}$ to approximate the solutions of Problem P_λ . In what follows, we first show the existence of a solution for Problem $P_{N\lambda}^{clos}$ that satisfies also the closure conditions (feasibility). Second, we investigate the convergence properties of this solution as $N \rightarrow \infty$ (consistency). Third, by combining these two results, we finally formulate the *covector mapping theorem* for Bernstein approximations, which provides a bijective map (covector mapping) between the solution of Problem $P_{N\lambda}^{clos}$ and the solution of Problem P_λ . The main results of this section are summarized in the three theorems below.

Theorem 3 (Feasibility) *Let*

$$\delta_D^N = C_D \max\{\delta_P^N, W_{\lambda'}(N^{-\frac{1}{2}}), W_\lambda(N^{-\frac{1}{2}}), W_\mu(N^{-\frac{1}{2}})\}, \quad (36)$$

where C_D is a positive constant independent of N , δ_P^N was defined in Equation (15), and $W_{\lambda'}(\cdot)$, $W_\lambda(\cdot)$, and $W_\mu(\cdot)$ are the moduli of continuity of $\dot{\lambda}(t)$, $\lambda(t)$ and $\mu(t)$, respectively. Then Problem $P_{N\lambda}^{clos}$ is feasible for arbitrary order of approximation $N \in \mathbb{Z}^+$. ■

Proof: Similar to the proof of Theorem 1, this proof follows by constructing a solution for Problem $P_{N\lambda}^{clos}$, with δ_D^N given by Equation (36). To this end, let $x(t)$, $u(t)$, $\lambda(t)$, $\mu(t)$ and ν be a solution of Problem P_λ , which exists by Assumption 4, and define

$$\bar{x}_{j,N} = x(t_j), \quad \bar{u}_{j,N} = u(t_j), \quad (37)$$

$$\bar{\lambda}_{j,N} = w\lambda(t_j), \quad \bar{\mu}_{j,N} = w\mu(t_j), \quad \bar{\nu} = \nu, \quad (38)$$

for all $j = 0, \dots, N$, $t_j = \frac{j}{N}$, $w = \frac{1}{N+1}$, with corresponding Bernstein polynomials given by

$$\mathbf{x}_N(t) = \sum_{j=0}^N \bar{x}_{j,N} b_{j,N}(t), \quad \mathbf{u}_N(t) = \sum_{j=0}^N \bar{u}_{j,N} b_{j,N}(t), \quad \lambda_N(t) = \sum_{j=0}^N \bar{\lambda}_{j,N} b_{j,N}(t), \quad \mu_N(t) = \sum_{j=0}^N \bar{\mu}_{j,N} b_{j,N}(t). \quad (39)$$

The remainder of this proof shows that $\mathbf{x}_N(t)$, $\mathbf{u}_N(t)$, $\lambda_N(t)$, $\mu_N(t)$ and $\bar{\nu}$ given above satisfy Equations (32)-(35) (we notice that the satisfaction of Equations (11)-(13) has already been addressed in the proof of Theorem 1). We start by defining the Bernstein coefficients $\tilde{\lambda}_{j,N}$ and $\tilde{\mu}_{j,N}$ as follows

$$\tilde{\lambda}_{j,N} = \frac{\bar{\lambda}_{j,N}}{w}, \quad \tilde{\mu}_{j,N} = \frac{\bar{\mu}_{j,N}}{w}, \quad (40)$$

with corresponding Bernstein polynomials given by

$$\tilde{\lambda}_N(t) = \sum_{j=0}^N \tilde{\lambda}_{j,N} b_{j,N}(t), \quad \tilde{\mu}_N(t) = \sum_{j=0}^N \tilde{\mu}_{j,N} b_{j,N}(t).$$

Notice that

$$\tilde{\lambda}_N(t) = \frac{\lambda_N(t)}{w}, \quad \tilde{\mu}_N(t) = \frac{\mu_N(t)}{w}. \quad (41)$$

Combining Equations (37), (38) and (40) and using Assumption 4 and Lemma 1, we get

$$\begin{aligned} \|\mathbf{x}_N(t) - \mathbf{x}(t)\| &\leq C_x W_x(N^{-\frac{1}{2}}), & \|\mathbf{u}_N(t) - \mathbf{u}(t)\| &\leq C_u W_u(N^{-\frac{1}{2}}), & \|\dot{\mathbf{x}}_N(t) - \dot{\mathbf{x}}(t)\| &\leq C_{x'} W_{x'}(N^{-\frac{1}{2}}), \\ \|\tilde{\lambda}_N(t) - \lambda(t)\| &\leq C_\lambda W_\lambda(N^{-\frac{1}{2}}), & \|\tilde{\mu}_N(t) - \mu(t)\| &\leq C_\mu W_\mu(N^{-\frac{1}{2}}), & \|\dot{\tilde{\lambda}}_N(t) - \dot{\lambda}(t)\| &\leq C_{\lambda'} W_{\lambda'}(N^{-\frac{1}{2}}), \end{aligned} \quad (42)$$

where $C_\lambda < \frac{5n_x}{4}$, $C_\mu < \frac{5n_u}{4}$, $C_{\lambda'} < \frac{9n_x}{4}$ and $W_\lambda(\cdot)$, $W_\mu(\cdot)$ and $W_{\lambda'}(\cdot)$ are the moduli of continuity of $\lambda(t)$, $\mu(t)$ and $\dot{\lambda}(t)$, respectively.

Now we show that the bound in Equation (32) is satisfied. Using Equation (41), and adding and subtracting $w(\boldsymbol{\mu}^\top(t_k)\mathbf{h}(\mathbf{x}_N(t_k), \mathbf{u}_N(t_k)) + \boldsymbol{\mu}^\top(t_k)\mathbf{h}(\mathbf{x}(t_k), \mathbf{u}(t_k)))$, we get

$$\begin{aligned} \|\boldsymbol{\mu}_N^\top(t_k)\mathbf{h}(\mathbf{x}_N(t_k), \mathbf{u}_N(t_k))\| &= \|w\tilde{\boldsymbol{\mu}}_N^\top(t_k)\mathbf{h}(\mathbf{x}_N(t_k), \mathbf{u}_N(t_k))\| \\ &\leq w\|(\tilde{\boldsymbol{\mu}}_N^\top(t_k) - \boldsymbol{\mu}^\top(t_k))\mathbf{h}(\mathbf{x}_N(t_k), \mathbf{u}_N(t_k))\| + w\|\boldsymbol{\mu}^\top(t_k)\mathbf{h}(\mathbf{x}(t_k), \mathbf{u}(t_k))\| \\ &\quad + w\|\boldsymbol{\mu}^\top(t_k)(\mathbf{h}(\mathbf{x}_N(t_k), \mathbf{u}_N(t_k)) - \mathbf{h}(\mathbf{x}(t_k), \mathbf{u}(t_k)))\| \end{aligned}$$

Using Equation (26), the above inequality reduces to

$$\begin{aligned} \|\boldsymbol{\mu}_N^\top(t_k)\mathbf{h}(\mathbf{x}_N(t_k), \mathbf{u}_N(t_k))\| &\leq w\|(\tilde{\boldsymbol{\mu}}_N^\top(t_k) - \boldsymbol{\mu}^\top(t_k))\mathbf{h}(\mathbf{x}_N(t_k), \mathbf{u}_N(t_k))\| \\ &\quad + w\|\boldsymbol{\mu}^\top(t_k)(\mathbf{h}(\mathbf{x}_N(t_k), \mathbf{u}_N(t_k)) - \mathbf{h}(\mathbf{x}(t_k), \mathbf{u}(t_k)))\| \\ &\leq w\|\mathbf{h}(\mathbf{x}_N(t_k), \mathbf{u}_N(t_k))\|C_\mu W_\mu(N^{-\frac{1}{2}}) \\ &\quad + w\|\boldsymbol{\mu}^\top(t_k)\|L_h(C_x W_x(N^{-\frac{1}{2}}) + C_u W_u(N^{-\frac{1}{2}})), \end{aligned}$$

where we used the bounds in Equation (42) together with the Lipschitz assumption on \mathbf{h} (see Assumptions 3). Finally, from using Assumptions 3 and 4, it follows that \mathbf{h} and $\boldsymbol{\mu}$ are bounded on $[0, 1]$ with bounds h_{\max} and μ_{\max} , respectively. Therefore, we get

$$\|\boldsymbol{\mu}_N^\top(t_k)\mathbf{h}(\mathbf{x}_N(t_k), \mathbf{u}_N(t_k))\| \leq w[h_{\max}C_\mu W_\mu(N^{-\frac{1}{2}}) + \mu_{\max}L_h(C_x W_x(N^{-\frac{1}{2}}) + C_u W_u(N^{-\frac{1}{2}}))],$$

which implies that the bound in Equation (32) is satisfied with δ_D^N given by Equation (36) and $C_D > h_{\max}C_\mu + \mu_{\max}L_h(C_x + C_u)$. Similarly,

$$\boldsymbol{\mu}_N(t_k) = w\tilde{\boldsymbol{\mu}}_N(t_k) \geq w\boldsymbol{\mu}(t_k) - w\|\boldsymbol{\mu}(t_k) - \tilde{\boldsymbol{\mu}}_N(t_k)\|\mathbf{1} \geq -N^{-1}C_\mu W_\mu(N^{-\frac{1}{2}})\mathbf{1},$$

which proves that Equation (32) holds.

Now consider the left equation in (33). For $k = 0$ we have

$$\begin{aligned} \left\| \frac{\partial \mathcal{L}_N}{\partial \bar{\mathbf{x}}_{0,N}} \right\| &= \left\| E_{x(0)}(\mathbf{x}_N(0), \mathbf{x}_N(t_N)) + w \sum_{j=0}^N F_x(\mathbf{x}_N(t_j), \mathbf{u}_N(t_j))b_{0,N}(t_j) \right. \\ &\quad \left. + \sum_{j=0}^N \boldsymbol{\lambda}_N^\top(t_j) \left[-\dot{b}_{0,N}(t_j) + \mathbf{f}_x(\mathbf{x}_N(t_j), \mathbf{u}_N(t_j))b_{0,N}(t_j) \right] \right. \\ &\quad \left. + \sum_{j=0}^N \boldsymbol{\mu}_N^\top(t_j)\mathbf{h}_x(\mathbf{x}_N(t_j), \mathbf{u}_N(t_j))b_{0,N}(t_j) + \bar{\mathbf{v}}^\top \mathbf{e}_{x(0)}(\mathbf{x}_N(0), \mathbf{x}_N(t_N)) \right\|. \end{aligned} \quad (43)$$

Substituting $w\tilde{\boldsymbol{\lambda}}_N(t_j) = \boldsymbol{\lambda}_N(t_j)$ and $w\tilde{\boldsymbol{\mu}}_N(t_j) = \boldsymbol{\mu}_N(t_j)$, the equation above can be written as

$$\begin{aligned} \left\| \frac{\partial \mathcal{L}_N}{\partial \bar{\mathbf{x}}_{0,N}} \right\| &= \left\| E_{x(0)}(\mathbf{x}_N(0), \mathbf{x}_N(t_N)) + w \sum_{j=0}^N F_x(\mathbf{x}_N(t_j), \mathbf{u}_N(t_j))b_{0,N}(t_j) \right. \\ &\quad \left. + w \sum_{j=0}^N \tilde{\boldsymbol{\lambda}}_N^\top(t_j) \left[-\dot{b}_{0,N}(t_j) + \mathbf{f}_x(\mathbf{x}_N(t_j), \mathbf{u}_N(t_j))b_{0,N}(t_j) \right] \right. \\ &\quad \left. + w \sum_{j=0}^N \tilde{\boldsymbol{\mu}}_N^\top(t_j)\mathbf{h}_x(\mathbf{x}_N(t_j), \mathbf{u}_N(t_j))b_{0,N}(t_j) + \bar{\mathbf{v}}^\top \mathbf{e}_{x(0)}(\mathbf{x}_N(0), \mathbf{x}_N(t_N)) \right\|. \end{aligned} \quad (44)$$

Notice that the following inequalities are satisfied:

$$\left\| w \sum_{j=0}^N F_x(\mathbf{x}_N(t_j), \mathbf{u}_N(t_j)) b_{0,N}(t_j) - \int_0^1 F_x(\mathbf{x}(t), \mathbf{u}(t)) b_{0,N}(t) dt \right\| \leq \bar{C}_1(N^{-\frac{1}{2}} + W_x(N^{-\frac{1}{2}}) + W_u(N^{-\frac{1}{2}})) \quad (45a)$$

$$\left\| w \sum_{j=0}^N \tilde{\lambda}_N^\top(t_j) \dot{b}_{0,N}(t_j) - \int_0^1 \lambda^\top(t) \dot{b}_{0,N}(t) dt \right\| \leq \bar{C}_2(N^{-\frac{1}{2}} + W_\lambda(N^{-\frac{1}{2}})) \quad (45b)$$

$$\left\| w \sum_{j=0}^N \tilde{\lambda}_N^\top(t_j) \mathbf{f}_x(\mathbf{x}_N(t_j), \mathbf{u}_N(t_j)) b_{0,N}(t_j) - \int_0^1 \lambda^\top(t) \mathbf{f}_x(\mathbf{x}(t), \mathbf{u}(t)) b_{0,N}(t) dt \right\| \leq \quad (45c)$$

$$\bar{C}_3(N^{-\frac{1}{2}} + W_\lambda(N^{-\frac{1}{2}}) + W_x(N^{-\frac{1}{2}}) + W_u(N^{-\frac{1}{2}}))$$

$$\left\| w \sum_{j=0}^N \tilde{\mu}_N^\top(t_j) \mathbf{h}_x(\mathbf{x}_N(t_j), \mathbf{u}_N(t_j)) b_{0,N}(t_j) - \int_0^1 \mu^\top(t) \mathbf{h}_x(\mathbf{x}(t), \mathbf{u}(t)) b_{0,N}(t) dt \right\| \leq \quad (45d)$$

$$\bar{C}_4(N^{-\frac{1}{2}} + W_\mu(N^{-\frac{1}{2}}) + W_x(N^{-\frac{1}{2}}) + W_u(N^{-\frac{1}{2}})),$$

for some positive \bar{C}_1 , \bar{C}_2 , \bar{C}_3 and \bar{C}_4 independent of N . A proof of the above inequalities is given in Appendix A. Then the combination of Equations (44) and (45) yields the following inequality

$$\left\| \frac{\partial \mathcal{L}_N}{\partial \bar{\mathbf{x}}_{0,N}} \right\| \leq \left\| E_{x(0)}(\mathbf{x}(0), \mathbf{x}(1)) + \int_0^1 F_x(\mathbf{x}(t), \mathbf{u}(t)) b_{0,N}(t) dt - \int_0^1 \lambda^\top(t) \dot{b}_{0,N}(t) dt \right.$$

$$\left. + \int_0^1 \lambda^\top(t) \mathbf{f}_x(\mathbf{x}(t), \mathbf{u}(t)) b_{0,N}(t) dt + \int_0^1 \mu^\top(t) \mathbf{h}_x(\mathbf{x}(t), \mathbf{u}(t)) b_{0,N}(t) dt + \bar{\nu}^\top \mathbf{e}_{x(0)}(\mathbf{x}(0), \mathbf{x}(1)) \right\|$$

$$+ \bar{C} \max \left\{ N^{-\frac{1}{2}}, W_x(N^{-\frac{1}{2}}), W_u(N^{-\frac{1}{2}}), W_\lambda(N^{-\frac{1}{2}}), W_\mu(N^{-\frac{1}{2}}) \right\}, \quad (46)$$

with $\bar{C} \geq 4 \max\{\bar{C}_1, \bar{C}_2, \bar{C}_3, \bar{C}_4\}$. Using integration by parts, we have $\int_0^1 \lambda^\top(t) \dot{b}_{0,N}(t) dt = -\int_0^1 \dot{\lambda}^\top(t) b_{0,N}(t) dt + [\lambda^\top(t) b_{0,N}(t)]_0^1$. Thus, since $b_{0,N}(0) = 1, b_{0,N}(1) = 0$, the above inequality becomes

$$\left\| \frac{\partial \mathcal{L}_N}{\partial \bar{\mathbf{x}}_{0,N}} \right\| \leq \left\| E_{x(0)}(\mathbf{x}(0), \mathbf{x}(1)) + \lambda^\top(0) + \bar{\nu}^\top \mathbf{e}_{x(0)}(\mathbf{x}(0), \mathbf{x}(1)) \right.$$

$$\left. + \int_0^1 \left[\dot{\lambda}^\top(t) + F_x(\mathbf{x}(t), \mathbf{u}(t)) + \lambda^\top(t) \mathbf{f}_x(\mathbf{x}(t), \mathbf{u}(t)) + \mu^\top(t) \mathbf{h}_x(\mathbf{x}(t), \mathbf{u}(t)) \right] b_{0,N}(t) dt \right\| \quad (47)$$

$$+ \bar{C} \max \left\{ N^{-\frac{1}{2}}, W_x(N^{-\frac{1}{2}}), W_u(N^{-\frac{1}{2}}), W_\lambda(N^{-\frac{1}{2}}), W_\mu(N^{-\frac{1}{2}}) \right\}.$$

Finally, using Equations (27) and (28), the above inequality reduces to the left condition in Equation (33) for $k = 0$, with δ_D^N given by Equation (36) and $C_D \geq \bar{C}$. The same condition for $k = 1, \dots, N$ can be shown to be satisfied using an identical argument. The stationarity condition in the right of Equation (33) can also be verified similarly, and the computations are thus omitted. To show that the closure condition (34) is satisfied we use the definitions in Equations (37) and (38) together with the end point values property of Bernstein polynomials, Property 1 in Section 2, which gives

$$\left\| \frac{\lambda_N^\top(0)}{w} + \bar{\nu}^\top \mathbf{e}_{x(0)}(\mathbf{x}_N(0), \mathbf{x}_N(t_N)) + E_{x(0)}(\mathbf{x}_N(0), \mathbf{x}_N(t_N)) \right\| \leq$$

$$\left\| \lambda^\top(0) + \bar{\nu}^\top \mathbf{e}_{x(0)}(\mathbf{x}(0), \mathbf{x}(1)) + E_{x(0)}(\mathbf{x}(0), \mathbf{x}(1)) \right\| = 0,$$

where the last equality follows from Equation (28). An identical argument can be used to show that the closure condition (35) holds, thus completing the proof of Theorem 3. ♠

Corollary 2 *If solutions $\mathbf{x}^*(t)$, $\mathbf{u}^*(t)$, $\boldsymbol{\lambda}^*(t)$, $\boldsymbol{\mu}^*(t)$ and $\boldsymbol{\nu}^*$ of Problem P_λ exist and satisfy $\dot{\mathbf{x}}^*(t) \in \mathcal{C}_{n_x}^2$, $\mathbf{u}^*(t) \in \mathcal{C}_{n_u}^2$, $\boldsymbol{\lambda}^*(t) \in \mathcal{C}_{n_x}^2$, and $\boldsymbol{\mu}^*(t) \in \mathcal{C}_{n_h}^2$ in $[0, 1]$, then Theorem 3 holds with $\delta_P^N = C_P N^{-1}$ and $\delta_D^N = C_D N^{-1}$, where C_P and C_D are positive constants independent of N .* ■

Proof: The proof of Corollary 2 follows easily by applying Lemma 2 to the proof of Theorem 3. ♠

Remark 4 *Similarly to Remark 2, for arbitrarily small scalar $\epsilon_D > 0$ there exists N_1 such that for all $N \geq N_1$, we have $\delta_D^N \leq \epsilon_D$; i.e., the relaxation bound in Problem $P_{N\lambda}^{\text{clos}}$ can be made arbitrarily small by choosing sufficiently large N .*

Theorem 4 (Consistency) *Let $\{(\bar{\mathbf{x}}_N^*, \bar{\mathbf{u}}_N^*, \bar{\boldsymbol{\lambda}}_N^*, \bar{\boldsymbol{\mu}}_N^*, \bar{\boldsymbol{\nu}}^*)\}_{N=N_1}^\infty$ be a sequence of solutions of Problem $P_{N\lambda}^{\text{clos}}$. Consider the sequence of transformed solutions $\{(\tilde{\mathbf{x}}_N^*, \tilde{\mathbf{u}}_N^*, \tilde{\boldsymbol{\lambda}}_N^*, \tilde{\boldsymbol{\mu}}_N^*, \tilde{\boldsymbol{\nu}}^*)\}_{N=N_1}^\infty$, with*

$$\tilde{\boldsymbol{\lambda}}_{j,N}^* = \frac{\bar{\boldsymbol{\lambda}}_{j,N}^*}{w}, \quad \tilde{\boldsymbol{\mu}}_{j,N}^* = \frac{\bar{\boldsymbol{\mu}}_{j,N}^*}{w},$$

and the corresponding polynomial approximation $\{(\mathbf{x}_N^(t), \mathbf{u}_N^*(t), \tilde{\boldsymbol{\lambda}}_N^*(t), \tilde{\boldsymbol{\mu}}_N^*(t), \tilde{\boldsymbol{\nu}}^*)\}_{N=N_1}^\infty$. Assume that the latter has a uniform accumulation point, i.e.*

$$\lim_{N \rightarrow \infty} (\mathbf{x}_N^*(t), \mathbf{u}_N^*(t), \tilde{\boldsymbol{\lambda}}_N^*(t), \tilde{\boldsymbol{\mu}}_N^*(t), \tilde{\boldsymbol{\nu}}^*) = (\mathbf{x}^\infty(t), \mathbf{u}^\infty(t), \tilde{\boldsymbol{\lambda}}^\infty(t), \tilde{\boldsymbol{\mu}}^\infty(t), \tilde{\boldsymbol{\nu}}^\infty), \quad \forall t \in [0, 1],$$

and assume $\dot{\mathbf{x}}^\infty(t)$, $\mathbf{u}^\infty(t)$, $\tilde{\boldsymbol{\lambda}}^\infty(t)$ and $\tilde{\boldsymbol{\mu}}^\infty(t)$ are continuous on $[0, 1]$. Then, $(\mathbf{x}^\infty(t), \mathbf{u}^\infty(t), \tilde{\boldsymbol{\lambda}}^\infty(t), \tilde{\boldsymbol{\mu}}^\infty(t), \tilde{\boldsymbol{\nu}}^\infty)$ is a solution of Problem P_λ . ■

Proof: The objective is to show that $\mathbf{x}^\infty(t)$, $\mathbf{u}^\infty(t)$, $\tilde{\boldsymbol{\lambda}}^\infty(t)$, $\tilde{\boldsymbol{\mu}}^\infty(t)$ and $\tilde{\boldsymbol{\nu}}^\infty$ satisfy Equations (6)-(8) and (26)-(30). The satisfaction of Equations (6)-(8) has been demonstrated in the proof of Theorem 2. We start by showing Equation (26), and we do so using a proof by contradiction. Assume that $\mathbf{x}^\infty(t)$, $\mathbf{u}^\infty(t)$, $\tilde{\boldsymbol{\mu}}^\infty(t)$ do not satisfy Equation (26). Then there exists $t' \in [0, 1]$, such that

$$\|\tilde{\boldsymbol{\mu}}^{\infty\top}(t') \mathbf{h}(\mathbf{x}^\infty(t'), \mathbf{u}^\infty(t'))\| > 0. \quad (48)$$

Since the nodes $\{t_k\}_{k=0}^N$ are dense in $[0, 1]$, there exists a sequence of indices $\{k_N\}_{N=0}^\infty$ such that

$$\lim_{N \rightarrow \infty} t_{k_N} = t',$$

which implies

$$\begin{aligned} \lim_{N \rightarrow \infty} \|\tilde{\boldsymbol{\mu}}^\infty(t') - \tilde{\boldsymbol{\mu}}^\infty(t_{k_N})\| &= 0, \\ \lim_{N \rightarrow \infty} \|\mathbf{x}^\infty(t') - \mathbf{x}^\infty(t_{k_N})\| &= 0, \\ \lim_{N \rightarrow \infty} \|\mathbf{u}^\infty(t') - \mathbf{u}^\infty(t_{k_N})\| &= 0. \end{aligned}$$

Then we have

$$\begin{aligned} \|\tilde{\boldsymbol{\mu}}^{\infty\top}(t') \mathbf{h}(\mathbf{x}^\infty(t'), \mathbf{u}^\infty(t'))\| &\leq \lim_{N \rightarrow \infty} \|(\tilde{\boldsymbol{\mu}}_N^{*\top}(t') - \tilde{\boldsymbol{\mu}}_N^{*\top}(t_{k_N})) \mathbf{h}(\mathbf{x}_N^*(t'), \mathbf{u}_N^*(t'))\| \\ &\quad + \lim_{N \rightarrow \infty} \|\tilde{\boldsymbol{\mu}}_N^{*\top}(t_{k_N}) (\mathbf{h}(\mathbf{x}_N^*(t'), \mathbf{u}_N^*(t')) - \mathbf{h}(\mathbf{x}_N^*(t_{k_N}), \mathbf{u}_N^*(t_{k_N})))\| \\ &\quad + \lim_{N \rightarrow \infty} \|\tilde{\boldsymbol{\mu}}_N^{*\top}(t_{k_N}) \mathbf{h}(\mathbf{x}_N^*(t_{k_N}), \mathbf{u}_N^*(t_{k_N}))\| \\ &= \lim_{N \rightarrow \infty} \frac{1}{w} \|\boldsymbol{\mu}_N^{*\top}(t_{k_N}) \mathbf{h}(\mathbf{x}_N^*(t_{k_N}), \mathbf{u}_N^*(t_{k_N}))\| = 0, \end{aligned}$$

where we used Equation (32). This contradicts Equation (48). Similarly, we can show that $\tilde{\boldsymbol{\mu}}^\infty(t) \geq 0$, thus proving that $\mathbf{x}^\infty(t)$, $\mathbf{u}^\infty(t)$ and $\tilde{\boldsymbol{\mu}}^\infty(t)$ satisfy Equation (26).

Furthermore, we notice that if $\mathbf{x}^\infty(t), \mathbf{u}^\infty(t), \tilde{\boldsymbol{\lambda}}^\infty(t), \tilde{\boldsymbol{\mu}}^\infty(t)$ and $\bar{\boldsymbol{\nu}}^\infty$ satisfy Equations (33)-(35), then the following holds for all $k = 0, \dots, N$:

$$\begin{aligned} & \left\| \tilde{\boldsymbol{\lambda}}^{\infty\top}(0) + \bar{\boldsymbol{\nu}}^{\infty\top} \mathbf{e}_{x(0)}(\mathbf{x}^\infty(0), \mathbf{x}^\infty(1)) + E_{x(0)}(\mathbf{x}^\infty(0), \mathbf{x}^\infty(1)) \right\| = 0, \\ & \left\| \boldsymbol{\lambda}^{\infty\top}(1) - \bar{\boldsymbol{\nu}}^{\infty\top} \mathbf{e}_{x(1)}(\mathbf{x}^\infty(0), \mathbf{x}^\infty(1)) - E_{x(1)}(\mathbf{x}^\infty(0), \mathbf{x}^\infty(1)) \right\| = 0, \\ & \left\| \int_0^1 \left[\dot{\tilde{\boldsymbol{\lambda}}^{\infty\top}}(t) + F_x(\mathbf{x}^\infty(t), \mathbf{u}^\infty(t)) + \tilde{\boldsymbol{\lambda}}^{\infty\top}(t) \mathbf{f}_x(\mathbf{x}^\infty(t), \mathbf{u}^\infty(t)) + \tilde{\boldsymbol{\mu}}^{\infty\top}(t) \mathbf{h}_x(\mathbf{x}^\infty(t), \mathbf{u}^\infty(t)) \right] b_{k,N}(t) dt \right\| = 0, \\ & \left\| \int_0^1 \left[F_u(\mathbf{x}^\infty(t), \mathbf{u}^\infty(t)) + \tilde{\boldsymbol{\lambda}}^{\infty\top}(t) \mathbf{f}_u(\mathbf{x}^\infty(t), \mathbf{u}^\infty(t)) + \tilde{\boldsymbol{\mu}}^{\infty\top}(t) \mathbf{h}_u(\mathbf{x}^\infty(t), \mathbf{u}^\infty(t)) \right] b_{k,N}(t) dt \right\| = 0. \end{aligned}$$

Since $\{b_{k,N}(t)\}_{k=0}^N$ is a linearly independent basis set, the last two equations above imply

$$\begin{aligned} & \left\| \dot{\tilde{\boldsymbol{\lambda}}^{\infty\top}}(t) + F_x(\mathbf{x}^\infty(t), \mathbf{u}^\infty(t)) + \tilde{\boldsymbol{\lambda}}^{\infty\top}(t) \mathbf{f}_x(\mathbf{x}^\infty(t), \mathbf{u}^\infty(t)) + \tilde{\boldsymbol{\mu}}^{\infty\top}(t) \mathbf{h}_x(\mathbf{x}^\infty(t), \mathbf{u}^\infty(t)) \right\| = 0, \\ & \left\| F_u(\mathbf{x}^\infty(t), \mathbf{u}^\infty(t)) + \tilde{\boldsymbol{\lambda}}^{\infty\top}(t) \mathbf{f}_u(\mathbf{x}^\infty(t), \mathbf{u}^\infty(t)) + \tilde{\boldsymbol{\mu}}^{\infty\top}(t) \mathbf{h}_u(\mathbf{x}^\infty(t), \mathbf{u}^\infty(t)) \right\| = 0, \end{aligned}$$

for all $t \in [0, 1]$. This proves that $\mathbf{x}^\infty(t), \mathbf{u}^\infty(t), \tilde{\boldsymbol{\lambda}}^\infty(t), \tilde{\boldsymbol{\mu}}^\infty(t)$ and $\bar{\boldsymbol{\nu}}^\infty(t)$ satisfy Equations (27)-(30). ♠

Theorem 5 (Covector Mapping Theorem) *Under the same assumptions of Theorems 3 and 4, when $N \rightarrow \infty$, the covector mapping*

$$\begin{aligned} \mathbf{x}_N^*(t) &\mapsto \mathbf{x}^*(t), & \mathbf{u}_N^*(t) &\mapsto \mathbf{u}^*(t), \\ \frac{\boldsymbol{\lambda}_N^*}{w} &\mapsto \boldsymbol{\lambda}^*(t), & \frac{\boldsymbol{\mu}_N^*(t)}{w} &\mapsto \boldsymbol{\mu}^*(t), & \bar{\boldsymbol{\nu}}^* &\mapsto \boldsymbol{\nu}^* \end{aligned}$$

is a bijective mapping between the solution of Problem $P_{N\lambda}^{clos}$ and the solution of Problem P_λ . ■

Proof: The above result follows directly from Theorems 3 and 4. ♠

8 Numerical examples

This section presents four numerical examples aimed at validating the convergence properties of the proposed method based on Bernstein approximation. In the first example we consider a non-linear one-dimensional optimal control problem with smooth state, input and costate. In the second example we investigate the applicability and efficacy of our approach, when solving a bang-bang optimal control problem. In the third and fourth examples we demonstrate the benefits of the proposed method, when solving trajectory generation problems for single-vehicle and multi-vehicle missions, respectively. The results are obtained using MATLAB's built in *fmincon* function.

8.1 Example 1

Consider the following optimal control problem taken from [37]:

Example 1 *Determine $y : [0, 5] \rightarrow \mathbb{R}$ and $u : [0, 5] \rightarrow \mathbb{R}$ that minimize*

$$I(y(t), u(t)) = \frac{1}{2} \int_0^5 (y(t) + u^2(t)) dt,$$

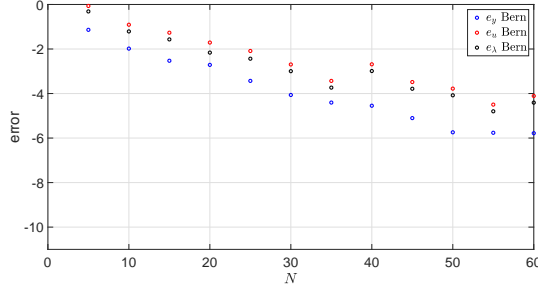


Figure 2: Error in Bernstein approximation method for Example 1.

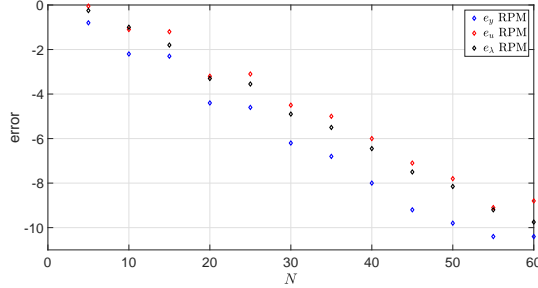


Figure 3: Error in Radau Pseudospectral Method (RPM) for Example 1 (taken from [37]).

subject to

$$\begin{aligned} \dot{y}(t) &= 2y(t) + 2u(t)\sqrt{y(t)}, \quad \forall t \in [0, 5], \\ y(0) &= 2, \\ y(5) &= 1. \end{aligned}$$

The above example was solved using the Bernstein approximation method for orders $N = 5, 10, \dots, 55, 60$. Similar to [37], we define the following errors

$$\begin{aligned} e_y &= \max_{k=0, \dots, N} \log_{10} |y_N^*(t_k) - y^*(t_k)|, \\ e_u &= \max_{k=0, \dots, N} \log_{10} |u_N^*(t_k) - u^*(t_k)|, \\ e_\lambda &= \max_{k=0, \dots, N} \log_{10} |\lambda_N^*(t_k) - \lambda^*(t_k)|, \end{aligned}$$

where $y_N^*(t_k)$, $u_N^*(t_k)$ and $\lambda_N^*(t_k)$ are the state, input and costate evaluated at the equidistant time nodes $t_k = 5k/N$, $k = 0, \dots, N$, while $y^*(t_k)$, $u^*(t_k)$ and $\lambda^*(t_k)$ are the exact solutions. Figure 2 illustrates the convergence of the above errors to zero as the order of approximation increases. As expected, the Bernstein approximation method is outperformed by pseudospectral methods in terms of converge rate. For example, Figure 3 presents the results obtained using the Radau Pseudospectral Method (RPM) presented in [37]. The data depicted in Figure 3 are reported from [37], where the authors solved Example 1 using RPM with the software OptimalPrime and the NLP solver SNOPT. Finally, Figure 4 depicts the state, input, and costate obtained using the Bernstein approximation method for order $N = 40$ alongside the exact solution.

8.2 Example 2 - Bang-bang control

This example investigates the efficacy of the proposed method when dealing with a bang-bang optimal control problem. Consider the following problem:

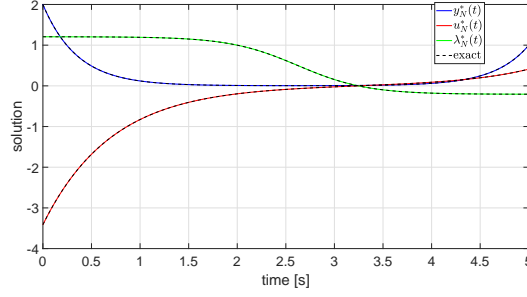


Figure 4: Solution to Example 1 using the Bernstein approximation method for order $N = 40$.

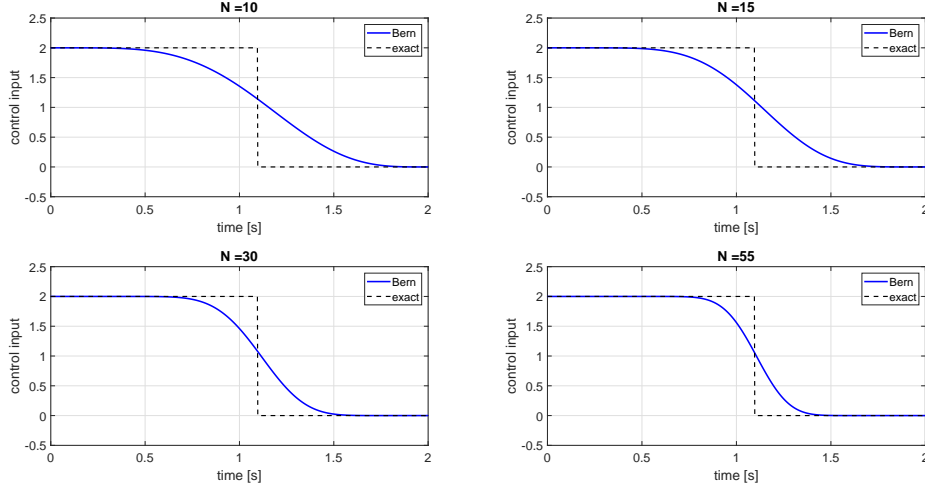


Figure 5: Solution to Example 2 using the Bernstein approximation method.

Example 2 Determine $y : [0, 2] \rightarrow \mathbb{R}$ and $u : [0, 2] \rightarrow \mathbb{R}$ that minimize

$$I(y(t), u(t)) = \int_0^2 (3u(t) - 2y(t))dt, \quad (49)$$

subject to

$$\dot{y}(t) = y(t) + u(t), \quad \forall t \in [0, 2], \quad (50)$$

$$y(0) = 4, \quad (51)$$

$$y(2) = 39.392, \quad (52)$$

$$0 \leq u(t) \leq 2 \quad \forall t \in [0, 2]. \quad (53)$$

The optimal control for the above example is:

$$u^*(t) = \begin{cases} 2 & 0 \leq t \leq 1.096 \\ 0 & 1.096 \leq t \leq 2. \end{cases}$$

Example 2 is solved using the Bernstein approximation method for orders of approximation $N = 10, 15, 30, 55$. The results are illustrated in Figure 5. It can be noted that the solutions resulting from the Bernstein approximation method converge, albeit slowly, to the exact solution, and behave nicely despite the discontinuity. The solutions have no jumps in the neighborhood of the discontinuities (the Gibbs phenomenon does not

occur for function approximation via Bernstein polynomials [24]), and the exact value of the discontinuity ($t = 1.096\text{s}$) is detected with reasonable accuracy even for low orders of approximation. The reader is referred to [20], where the discretization method presented in [40] is implemented to solve Example 2, emphasizing the inefficacy of pseudospectral methods when approximating bang-bang solutions. Additional references discussing the performance of pseudospectral methods when dealing with bang-bang optimal control problems can be found in [19, 21, 22, 41].

8.3 Example 3 - Trajectory generation for a single vehicle

In this section, the 2D trajectory generation problem for a single vehicle is considered. The vehicle, modelled as a single integrator, is required to navigate from the initial position $\mathbf{x}_0 = [-500, -900]\text{m}$ to the final destination $\mathbf{x}_f = [1500, -600]\text{m}$, while minimizing the time of arrival. The algorithm must ensure a minimum separation of $E = 50\text{m}$ with three obstacles positioned at $\mathbf{p}_{o_1} = [0 - 800]^\top\text{m}$, $\mathbf{p}_{o_2} = [450 - 750]^\top\text{m}$ and $\mathbf{p}_{o_3} = [850 - 730]^\top\text{m}$. Finally, the norm of the input must remain within minimum and maximum saturation limits $u_{\min} = 15\text{m/s}$ and $u_{\max} = 32\text{m/s}$. This problem can be formally stated as follows:

Example 3 Determine $\mathbf{x}(t)$, $\mathbf{u}(t)$ and t_f that minimize

$$I(\mathbf{x}(t), \mathbf{u}(t)) = \int_0^{t_f} dt,$$

subject to

$$\begin{aligned} \dot{\mathbf{x}}(t) &= \mathbf{u}(t), \quad \forall t \in [0, t_f], \\ \mathbf{x}(0) &= \mathbf{x}_0, \quad \mathbf{x}(t_f) = \mathbf{x}_f, \\ \|\mathbf{x}(t) - \mathbf{p}_{o_i}\| &\geq E, \quad \forall t \in [0, t_f], \quad i = 1, 2, 3, \\ u_{\min} &\leq \|\mathbf{u}(t)\| \leq u_{\max}, \quad \forall t \in [0, t_f]. \end{aligned}$$

The discretization method proposed in this paper is compared to the Legendre pseudospectral method [42]. The results are enclosed in Figure 6. The top-left, top-center and bottom-left figures show the trajectories, obtained using the pseudospectral method with orders of approximation 5, 20 and 100, respectively. As discussed in the introduction, the pseudospectral method enforces the constraints only at the discretization nodes and not in between them. By increasing the number of nodes, the distance between the entire trajectory and the obstacles increases towards the desired value $E = 50\text{m}$. However, as demonstrated by the top-right figure, which depicts the distance between the trajectories and the obstacles for the three order of approximations indicated above, the minimum separation constraint is never satisfied. On the other hand, the bottom-center figure shows that with the proposed method, even by choosing a small number of nodes ($N=5$ in this example), the collision avoidance constraint can be computed for the entire curve using, for example, the minimum distance algorithm introduced in Section 2, Property 4. Thus, collision avoidance is satisfied for the entire trajectory. The bottom-right figure supports this claim by showing that the distance between the trajectory and the obstacles is always greater than the required value.

8.4 Example 4 - Trajectory generation for multi-vehicle missions

As evidenced by the previous example, the possibility of choosing low order of approximations while guaranteeing constraint satisfaction is the strength of the proposed approach, which prioritizes safety and feasibility of the trajectories over optimality. The advantage of the method becomes more evident in multi-vehicle missions, where the trajectories assigned to the vehicles must be (spatially or temporally)¹ separated. Consider for example a mission scenario in which n vehicles, starting from their initial positions, have to follow spatially separated trajectories to reach predefined final destinations. By adopting the pseudospectral method described above, spatial separation would have to be enforced by imposing separation constraints between

¹Spatial separation is guaranteed if the minimum distance between any two points on two paths is greater than or equal to a minimum spatial clearance (the paths never intersect); temporal separation is achieved if for any time t the minimum distance between two vehicles is greater than or equal to the minimum spatial clearance.

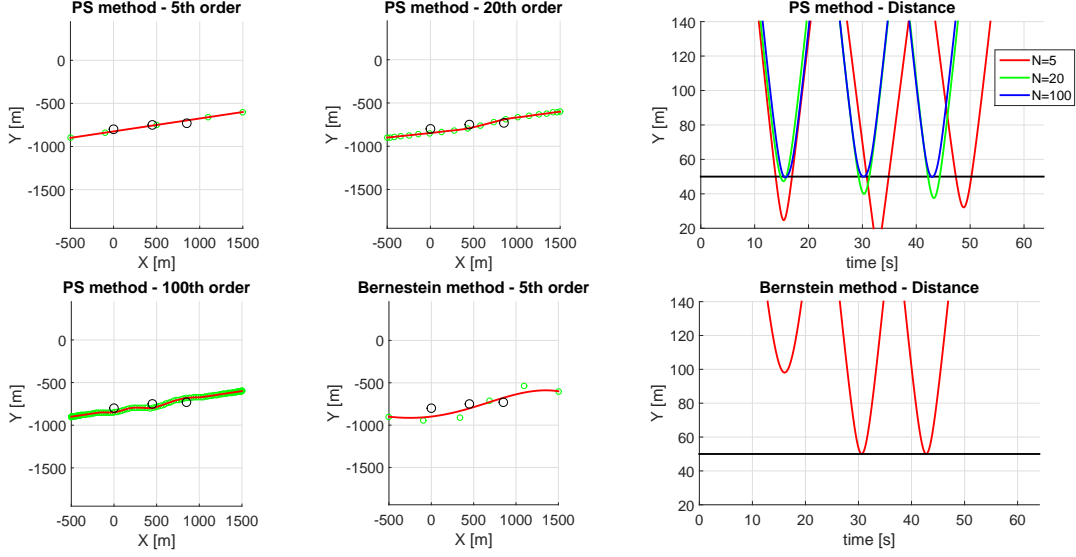


Figure 6: Legendre pseudospectral vs Bernstein approximation method: collision avoidance with multiple obstacles.

every node of every trajectory. Thus, the problem would have $\binom{n}{2} N^2$ separation constraints, where N is the number of nodes, and $\binom{n}{2}$ is the binomial coefficient. An increased number of nodes (dictated, perhaps, by reasons similar to the ones discussed in the previous example) would increase the complexity in the search for the optimal solution, making the pseudospectral approach practically infeasible for these types of applications. On the other hand, with the approach of this paper the constraint satisfaction is achieved independently of the number of nodes. This is discussed in the next simulation scenario.

Figure 7 illustrates the results of a multi-vehicle mission in which $n = 11$ vehicles, starting from their initial positions, have to reach a ‘>’ shaped formation while minimizing the time of arrival. The Bernstein approximation method is employed with the order of approximation $N = 8$. The dynamics of the i th vehicle are governed by the following differential equations

$$\begin{cases} \dot{x}_{1,i}(t) &= V_i(t) \cos(x_{3,i}(t)) \\ \dot{x}_{2,i}(t) &= V_i(t) \sin(x_{3,i}(t)) \\ \dot{x}_{3,i}(t) &= \omega_i(t), \end{cases} \quad (54)$$

with input $\mathbf{u}_i(t) = [V_i(t), \omega_i(t)]^\top$ and state $\mathbf{x}_i(t) = [x_{1,i}(t), x_{2,i}(t), x_{3,i}(t)]^\top$. The input constraints are:

$$V_{\min}^2 \leq V_i^2(t) \leq V_{\max}^2, \quad (55)$$

$$-\omega_{\max} \leq \omega_i(t) \leq \omega_{\max}, \quad (56)$$

with $V_{\min} = 15\text{m/s}$, $V_{\max} = 32\text{m/s}$ and $\omega_{\max} = 0.3\text{rad/s}$. Finally, temporal separation constraints are imposed between each pair of trajectories, i.e.

$$\|\mathbf{p}_i(t) - \mathbf{p}_j(t)\| \geq E, \quad (57)$$

$\forall i, j = 1, \dots, 11, i \neq j, \forall t \in [0, t_f]$, where $E = 50\text{m}$ and $\mathbf{p}_i(t) = [x_{1,i}(t), x_{2,i}(t)]^\top$.

The constraints in Equations (55), (56) and (57) are computed by exploiting the properties of Bernstein polynomials. In particular, we used the minimum distance and the computation of extrema algorithms from [16, 26]. Figures 8 and 9 show the time history of the speeds and angular rates, respectively, demonstrating that the input saturation constraints are satisfied for all times.

At last, the same simulation is repeated, but the temporal separation constraint given by Equation (57) is replaced by the (more stringent) spatial separation requirement

$$\|\mathbf{p}_i(t_k) - \mathbf{p}_j(t_p)\| \geq E, \quad (58)$$

$\forall i, j = 1, \dots, 11, i \neq j \forall t_k, t_p \in [0, t_f]$. Figure 10 depicts the 2D trajectories. Figures 11 and 12 illustrate the speed and angular rate commands, respectively.

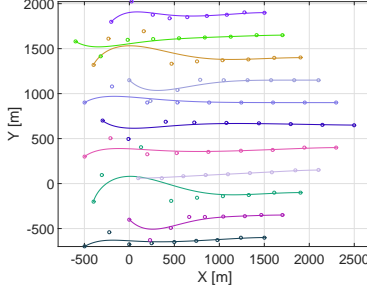


Figure 7: Multiple vehicles mission - temporal separation: 2D paths.

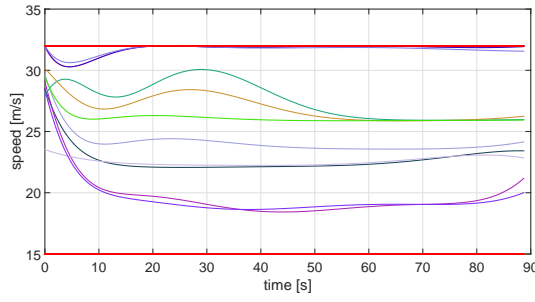


Figure 8: Multiple vehicles mission - temporal separation: speed profiles.

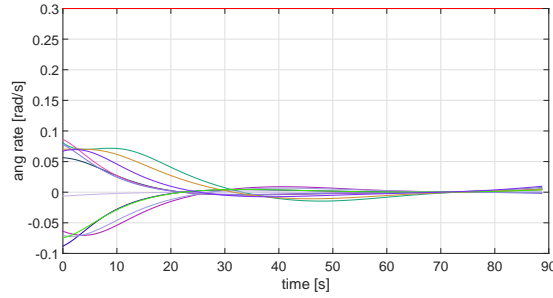


Figure 9: Multiple vehicles mission - temporal separation: angular rates.

9 Conclusions

This paper proposed a numerical method to approximate nonlinear constrained optimal control problems by nonlinear programming (NLPs) using Bernstein polynomial approximation. A rigorous analysis is provided that shows convergence of the solution of the NLP to the solution of the continuous-time problem. A set of

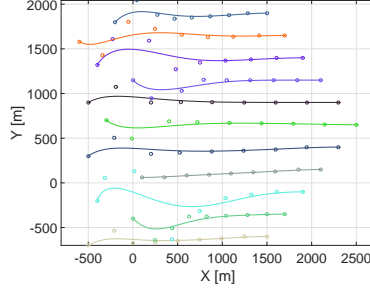


Figure 10: Multiple vehicles mission - spatial separation: 2D paths.

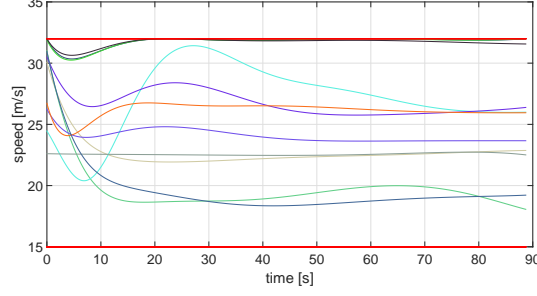


Figure 11: Multiple vehicles mission - spatial separation: speed profiles.

conditions are derived under which the Karush-Kuhn-Tucker multipliers of the NLP converge to the costates of the optimal control problem. This led to the formulation of the Covector Mapping Theorem for Bernstein approximation, which enables numerical computation of the costates. The theoretical findings are validated through several numerical examples, and the advantages and disadvantages of the proposed method are discussed.

Appendix

A Proof of Equation (45)

Let us focus on Equation (45a). Adding and subtracting $\int_0^1 F_x(\mathbf{x}_N(t), \mathbf{u}_N(t))b_{0,N}(t)dt$, we have

$$\begin{aligned}
& \left\| w \sum_{j=0}^N F_x(\mathbf{x}_N(t_j), \mathbf{u}_N(t_j))b_{0,N}(t_j) - \int_0^1 F_x(\mathbf{x}(t), \mathbf{u}(t))b_{0,N}(t)dt \right\| \leq \\
& \left\| w \sum_{j=0}^N F_x(\mathbf{x}_N(t_j), \mathbf{u}_N(t_j))b_{0,N}(t_j) - \int_0^1 F_x(\mathbf{x}_N(t), \mathbf{u}_N(t))b_{0,N}(t)dt + \int_0^1 F_x(\mathbf{x}_N(t), \mathbf{u}_N(t))b_{0,N}(t)dt \right. \\
& \quad \left. - \int_0^1 F_x(\mathbf{x}(t), \mathbf{u}(t))b_{0,N}(t)dt \right\| \tag{59} \\
& \leq \left\| w \sum_{j=0}^N F_x(\mathbf{x}_N(t_j), \mathbf{u}_N(t_j))b_{0,N}(t_j) - \int_0^1 F_x(\mathbf{x}_N(t), \mathbf{u}_N(t))b_{0,N}(t)dt \right\| \\
& \quad + \left\| \int_0^1 F_x(\mathbf{x}_N(t), \mathbf{u}_N(t))b_{0,N}(t)dt - \int_0^1 F_x(\mathbf{x}(t), \mathbf{u}(t))b_{0,N}(t)dt \right\|.
\end{aligned}$$

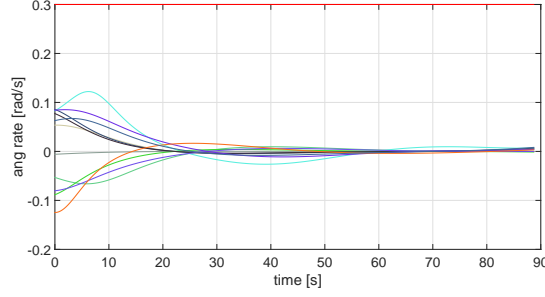


Figure 12: Multiple vehicles mission - spatial separation: angular rates.

Using Lemma 3 and continuity of $F_x(\mathbf{x}_N(t), \mathbf{u}_N(t))$ and $b_{0,N}(t)$, the first term on the right hand side of the inequality above satisfies

$$\left\| w \sum_{j=0}^N F_x(\mathbf{x}_N(t_j), \mathbf{u}_N(t_j)) b_{0,N}(t_j) - \int_0^1 F_x(\mathbf{x}_N(t), \mathbf{u}_N(t)) b_{0,N}(t) dt \right\| \leq C_I W_{F_x b_{0,N}}(N^{-\frac{1}{2}}),$$

where $W_{F_x b_{0,N}}(\cdot)$ is used to denote the modulus of continuity of the product $F_x(\mathbf{x}_N(t), \mathbf{u}_N(t)) b_{0,N}(t)$, with $F_x(\mathbf{x}_N(t), \mathbf{u}_N(t))$ being a bounded function due to its continuity over a bounded domain. Denote its bound as $F_{x,\max}$. Notice that also $b_{0,N}(t)$ is bounded, as $\max_{t \in [0,1]} b_{0,N}(t) \leq 1$. Then using the properties of the modulus of continuity, we get

$$\begin{aligned} \left\| w \sum_{j=0}^N F_x(\mathbf{x}_N(t_j), \mathbf{u}_N(t_j)) b_{0,N}(t_j) - \int_0^1 F_x(\mathbf{x}_N(t), \mathbf{u}_N(t)) b_{0,N}(t) dt \right\| &\leq C_I F_{x,\max} W_{b_{0,N}}(N^{-\frac{1}{2}}) + C_I W_{F_x}(N^{-\frac{1}{2}}) \\ &\leq C_I F_{x,\max} N^{-\frac{1}{2}} + C_I W_{F_x}(N^{-\frac{1}{2}}), \end{aligned} \quad (60)$$

where $W_{F_x}(\cdot)$ is the modulus of continuity of F_x , and C_I is a positive constant independent of N . Furthermore, we have

$$\begin{aligned} &\left\| \int_0^1 F_x(\mathbf{x}_N(t), \mathbf{u}_N(t)) b_{0,N}(t) dt - \int_0^1 F_x(\mathbf{x}(t), \mathbf{u}(t)) b_{0,N}(t) dt \right\| \\ &\leq \int_0^1 \|F_x(\mathbf{x}_N(t), \mathbf{u}_N(t)) b_{0,N}(t) - F_x(\mathbf{x}(t), \mathbf{u}(t)) b_{0,N}(t)\| dt \leq L_{F_x} (C_x W_x(N^{-\frac{1}{2}}) + C_u W_u(N^{-\frac{1}{2}})), \end{aligned} \quad (61)$$

where L_{F_x} is the Lipschitz constant of F_x , $C_x < 5n_x/4$, $C_u < 5n_u/4$, and $W_x(\cdot)$ and $W_u(\cdot)$ are the moduli of continuity of \mathbf{x} and \mathbf{u} , respectively. Combining Equations (60) and (61) with Equation (59), yields

$$\begin{aligned} &\left\| w \sum_{j=0}^N F_x(\mathbf{x}_N(t_j), \mathbf{u}_N(t_j)) b_{0,N}(t_j) - \int_0^1 F_x(\mathbf{x}(t), \mathbf{u}(t)) b_{0,N}(t) dt \right\| \\ &\leq C_I F_{x,\max} N^{-\frac{1}{2}} + C_I W_{F_x}(N^{-\frac{1}{2}}) + L_{F_x} (C_x W_x(N^{-\frac{1}{2}}) + C_u W_u(N^{-\frac{1}{2}})), \end{aligned} \quad (62)$$

which proves the bound in Equation (45a). The bounds in Equations (45b)-(45d) follow easily using an identical argument.

References

- [1] A. V. Rao, “A survey of numerical methods for optimal control,” *Advances in the Astronautical Sciences*, vol. 135, no. 1, pp. 497–528, 2009.
- [2] J. T. Betts, *Practical methods for optimal control and estimation using nonlinear programming*. SIAM, 2010.
- [3] —, “Survey of numerical methods for trajectory optimization,” *Journal of guidance, control, and dynamics*, vol. 21, no. 2, pp. 193–207, 1998.
- [4] B. A. Conway, “A survey of methods available for the numerical optimization of continuous dynamic systems,” *Journal of Optimization Theory and Applications*, vol. 152, no. 2, pp. 271–306, 2012.

- [5] E. Polak, “Optimization: Algorithms and consistent approximations,” 1997.
- [6] A. Schwartz and E. Polak, “Consistent approximations for optimal control problems based on runge–kutta integration,” *SIAM Journal on Control and Optimization*, vol. 34, no. 4, pp. 1235–1269, 1996.
- [7] I. M. Ross and M. Karpenko, “A review of pseudospectral optimal control: From theory to flight,” *Annual Reviews in Control*, vol. 36, no. 2, pp. 182–197, 2012.
- [8] F. Fahroo and I. M. Ross, “On discrete-time optimality conditions for pseudospectral methods,” in *AIAA/AAS Astrodynamics Specialist Conference and Exhibit*, 2006, p. 6304.
- [9] K. Bollino, L. R. Lewis, P. Sekhavat, and I. M. Ross, “Pseudospectral optimal control: a clear road for autonomous intelligent path planning,” in *AIAA Infotech@ Aerospace 2007 Conference and Exhibit*, 2007, p. 2831.
- [10] Q. Gong, R. Lewis, and M. Ross, “Pseudospectral motion planning for autonomous vehicles,” *Journal of Guidance, Control, and Dynamics*, vol. 32, no. 3, pp. 1039–1045, 2009.
- [11] N. S. Bedrossian, S. Bhatt, W. Kang, and I. M. Ross, “Zero-propellant maneuver guidance,” *IEEE Control Systems*, vol. 29, no. 5, 2009.
- [12] K. Bollino and L. R. Lewis, “Collision-free multi-uav optimal path planning and cooperative control for tactical applications,” in *AIAA Guidance, Navigation and Control Conference and Exhibit*, 2008, p. 7134.
- [13] N. Bedrossian, S. Bhatt, M. Lammers, L. Nguyen, and Y. Zhang, “First ever flight demonstration of zero propellant maneuver (tm) attitude control concept,” in *AIAA Guidance, Navigation and Control Conference and Exhibit*, 2007, p. 6734.
- [14] Y. Chen, M. Cutler, and J. P. How, “Decoupled multiagent path planning via incremental sequential convex programming,” in *Robotics and Automation (ICRA), 2015 IEEE International Conference on*. IEEE, 2015, pp. 5954–5961.
- [15] F. Augugliaro, A. P. Schoellig, and R. D’Andrea, “Generation of collision-free trajectories for a quadcopter fleet: A sequential convex programming approach,” in *Intelligent Robots and Systems (IROS), 2012 IEEE/RSJ International Conference on*. IEEE, 2012, pp. 1917–1922.
- [16] R. Choe, “Distributed cooperative trajectory generation for multiple autonomous vehicles using Pythagorean Hodograph Bézier curves,” Ph.D. dissertation, University of Illinois at Urbana-Champaign, Urbana, IL, United States, 2017, submitted.
- [17] V. Cichella, I. Kaminer, C. Walton, and N. Hovakimyan, “Optimal motion planning for differentially flat systems using Bernstein approximation,” *IEEE Control Systems Letters*, vol. 2, no. 1, pp. 181–186, 2018.
- [18] E. Hewitt and R. E. Hewitt, “The Gibbs-Wilbraham phenomenon: an episode in fourier analysis,” *Archive for history of Exact Sciences*, vol. 21, no. 2, pp. 129–160, 1979.
- [19] A. Gelb and J. Tanner, “Robust reprojection methods for the resolution of the gibbs phenomenon,” *Applied and Computational Harmonic Analysis*, vol. 20, no. 1, pp. 3–25, 2006.
- [20] E. Tohidi, A. Pasban, A. Kilicman, and S. L. Noghabi, “An efficient pseudospectral method for solving a class of nonlinear optimal control problems,” in *Abstract and Applied Analysis*, vol. 2013. Hindawi, 2013.
- [21] I. M. Ross and F. Fahroo, “Pseudospectral knotting methods for solving nonsmooth optimal control problems,” *Journal of Guidance, Control, and Dynamics*, vol. 27, no. 3, pp. 397–405, 2004.
- [22] C. L. Darby, W. W. Hager, and A. V. Rao, “An hp-adaptive pseudospectral method for solving optimal control problems,” *Optimal Control Applications and Methods*, vol. 32, no. 4, pp. 476–502, 2011.
- [23] R. T. Farouki, “The Bernstein polynomial basis: a centennial retrospective,” *Computer Aided Geometric Design*, vol. 29, no. 6, pp. 379–419, 2012.
- [24] H. Gzyl and J. L. Palacios, “On the approximation properties of Bernstein polynomials via probabilistic tools,” *Boletín de la Asociación Matemática Venezolana*, vol. 10, no. 1, pp. 5–13, 2003.
- [25] L. A. Ricciardi and M. Vasile, “Direct transcription of optimal control problems with finite elements on Bernstein basis,” *Journal of Guidance, Control and Dynamics*, 2018.
- [26] J.-W. Chang, Y.-K. Choi, M.-S. Kim, and W. Wang, “Computation of the minimum distance between two Bézier curves/surfaces,” *Computers & Graphics*, vol. 35, no. 3, pp. 677–684, 2011.
- [27] P. J. Davis, “Interpolation and approximation,” *Blaisdell Pub, Co., New York*, vol. 1, 1963.
- [28] S. N. Bernstein, “Démonstration du théorème de Weierstrass fondée sur le calcul des probabilités (demonstration of a theorem of Weierstrass based on the calculus of probabilities),” *Communications de la Société Mathématique de Kharkov*, vol. 13, no. 1, pp. 1–2, 1912.

- [29] R. Bojanic and F. Cheng, “Rate of convergence of Bernstein polynomials for functions with derivatives of bounded variation,” *Journal of Mathematical Analysis and Applications*, vol. 141, no. 1, pp. 136–151, 1989.
- [30] T. Popoviciu, “Sur l’approximation des fonctions convexes d’ordre supérieur,” *Mathematica (Cluj)*, vol. 10, pp. 49–54, 1935.
- [31] P. Sikkema, “Der wert einiger konstanten in der theorie der approximation mit bernstein-polynomen,” *Numerische Mathematik*, vol. 3, no. 1, pp. 107–116, 1961.
- [32] M. J. D. Powell, *Approximation theory and methods*. Cambridge university press, 1981.
- [33] M. S. Floater, “On the convergence of derivatives of Bernstein approximation,” *Journal of Approximation Theory*, vol. 134, no. 1, pp. 130–135, 2005.
- [34] E. G. Gilbert, D. W. Johnson, and S. S. Keerthi, “A fast procedure for computing the distance between complex objects in three-dimensional space,” *IEEE Journal on Robotics and Automation*, vol. 4, no. 2, pp. 193–203, 1988.
- [35] R. Choe, “Distributed cooperative trajectory generation for multiple autonomous vehicles using pythagorean hodograph Bézier curves,” Ph.D. dissertation, University of Illinois at Urbana-Champaign, 2017.
- [36] R. F. Hartl, S. P. Sethi, and R. G. Vickson, “A survey of the maximum principles for optimal control problems with state constraints,” *SIAM review*, vol. 37, no. 2, pp. 181–218, 1995.
- [37] D. Garg, M. A. Patterson, C. Francolin, C. L. Darby, G. T. Huntington, W. W. Hager, and A. V. Rao, “Direct trajectory optimization and costate estimation of finite-horizon and infinite-horizon optimal control problems using a radau pseudospectral method,” *Computational Optimization and Applications*, vol. 49, no. 2, pp. 335–358, 2011.
- [38] Q. Gong, I. M. Ross, W. Kang, and F. Fahroo, “Connections between the covector mapping theorem and convergence of pseudospectral methods for optimal control,” *Computational Optimization and Applications*, vol. 41, no. 3, pp. 307–335, 2008.
- [39] B. Singh, R. Bhattacharya, and S. R. Vadali, “Verification of optimality and costate estimation using hilbert space projection,” *Journal of guidance, control, and dynamics*, vol. 32, no. 4, pp. 1345–1355, 2009.
- [40] E. Tohidi, O. R. N. Samadi, and M. H. Farahi, “Legendre approximation for solving a class of nonlinear optimal control problems,” *Journal of Mathematical Finance*, vol. 1, no. 01, p. 8, 2011.
- [41] W. Kang, Q. Gong, and I. M. Ross, “Convergence of Pseudospectral Methods for a Class of Discontinuous Optimal Control,” in *2005 IEEE 44th Conference on Decision and Control (CDC)*, Seville, Spain, 2005, pp. 2799–2804.
- [42] Q. Gong, W. Kang, N. S. Bedrossian, F. Fahroo, P. Sekhavat, and K. Bollino, “Pseudospectral optimal control for military and industrial applications,” in *Decision and Control, 2007 46th IEEE Conference on*. IEEE, 2007, pp. 4128–4142.